Electronic Supplementary Information

Structural properties and influence of solvent in the stability of telomeric four-stranded i-motif DNA

Manas Mondal[1,2], Dhananjay Bhattacharyya[3], Yi Qin Gao[1, 2]*

[1]*Institute of Theoretical and Computational Chemistry, College of Chemistry and Molecular Engineering, Beijing National Laboratory for Molecular Sciences, Peking University, Beijing 100871, China*

[2]*BIOPIC, Peking University, Beijing 100871, China*

[3]*Computational Science Division, Saha Institute of Nuclear Physics,1/AF Bidhannagar, Kolkata 700064, India*

*Corresponding authors:

E-mail: gaoyq@pku.edu.cn

Table and Figure legends:

Table S1: Base pair orientational parameters in model $C^+C^+C^+$/CCC trinucleotide structure (ABC/DEF) as derived from the NMR structure of i-motif DNA (PDB id: 1EL2).

Table S2: Configurational entropy of the core and loop regions of the i-motif in 3'E and 5'E-form structure with hemi-protonated cytosines, derived from the normal mode analysis of equilibrated MD simulated trajectory at 300K.

Table S3: Average value along with standard deviation of the base pair parameters as found in experimental dataset and MD simulation of 3'E and 5'E-form structure under acidic pH with hemi-protonated cytosines having two different topologies.

Table S4: Average value along with standard deviation of the backbone dihedral angles for the bases as found in MD simulation of 5'E-form i-motif structure under acidic pH with hemi-protonated cytosines.

Table S5: Average value along with standard deviation of the backbone dihedral angles for the bases as found in MD simulation of 3'E-form i-motif structure under acidic pH with hemi-protonated cytosines.

Table S6: Average value along with standard deviation of the base pair parameters as found in MD simulation of 5'E-form structure in deprotonated state with normal cytosines.

Table S7: Average value along with standard deviation of the backbone dihedral angles for the bases as found in MD simulation of 5'E-form structure in deprotonated state with normal cytosines.

Table S8: Average hydrogen bonding geometry and occupancy (considering C – O distance ≤ 3.4 Å and C-H...O angle > 120°) of possible C-H...O mediated hydrogen bond between sugar moieties of the antiparallel strands along the narrow grooves of i-motif DNA.

Table S9: Base pairing and stacking energy between the stacked base pairs in model $C^+C^+C^+$/CCC trinucleotide structure (ABC/DEF) as derived from the NMR structure of i-motif DNA (PDB id: 1EL2).

Table S10: Variation of stacking energy between the stacked base pairs in model $C^{+}C^{+}C^{+}/CCC$ trinucleotide structure (ABC/DEF) with stacking interval between the consecutive base pairs.

Table S11: Average hydrogen bonding geometry and occupancy (considering C – O distance ≤ 3.4 Å and C-H...O angle > 120°) of possible C-H...O mediated hydrogen bond between sugar moieties of the antiparallel strands along the narrow grooves of i-motif DNA at elevated temperatures.

Table S12: Average value along with standard deviation of the base pair step parameters as found in MD simulation of 5’E_{GCC} and 5’E_{CGG} form structure (‘:’ denotes base pair and ‘::’ denotes base pairs stack).

Table S13: Average value along with standard deviation of stacking interval and twist between consecutive stacked base pair within i-motif core as found in MD simulation of 5’E_{GCC} and 5’E_{CGG}-form structure (‘:’ denotes base pair and ‘::’ denotes base pairs stack).

Table S14: Average value along with standard deviation of the backbone dihedral angles for the bases as found in MD simulation of 5’E_{GCC}-form structure.

Table S15: Average value along with standard deviation of the backbone dihedral angles for the bases as found in MD simulation of 5’E_{CGG}-form structure.

Table S16: Average hydrogen bonding geometry and occupancy (considering C – O distance ≤ 3.4 Å and C-H...O angle > 120°) of possible C-H...O mediated hydrogen bond between sugar moieties of the antiparallel strands along the narrow grooves of 5'E_{GCC} and 5'E_{CGG} i-motif DNA.

Fig. S1: Variation of RMSD with respect to the initial energy minimized structure in case of studied i-motif systems: (a) 3’E-form structure with hemi-protonated cytosines and normal cytosines at 300K, (b) 3’E-form structure with hemi-protonated cytosines at elevated temperatures, (c) 5’E-form structure with hemi-protonated cytosines and normal cytosines at 300K, (d) 5’E-form structure with hemi-protonated cytosines at elevated temperatures, (e) 5’E_{GCC} and 5’E_{CGG}-form structure with hemi-protonated cytosines at 300K and (f) 5’E-form structure with hemi-protonated cytosines and normal cytosine at 300K with TIP3P water model.

Fig. S2: Representative backbone refined conformations of model (a)-(h) $C^+C^+C^+$/CCC trinucleotide structures having different rotational orientation of intercalated base pair about its base pair helix axis and (i)-(p) tetranucleotide structures of two intercalated C^+C^+/CC dinuceotides with different helical rotations around their base pair helix axis.

Fig. S3: Root mean square fluctuation (RMSF) of the nucleotides in (a) 3’E and (b) 5’E-form i-motif structure under acidic pH with hemi-protonated cytosines.

Fig. S4: Distribution of distance between the N3 atoms of paired bases in equilibrated MD trajectory of 3’E (a) and 5’E-form (b) i-motif structure with hemi-protonated cytosines, and distance matrix for the nucleobases in equilibrated conformation of 3’E (c) and 5’E-form (d) i-motif structure with hemi-protonated cytosines.

Fig. S5: Variation of distance between the N3 atoms of paired bases along the MD simulated trajectory of 3’E (a)-(b) and 5’E-form (c)-(d) structure in deprotonated state with normal cytosines.

Fig. S6: Average conformation of (a) 3’E and (b) 5’E-form structure, and distance matrix for the nucleobases in equilibrated conformation of (c) 3’E and (d) 5’E-form structure under neutral pH with deprotonated cytosines.

Fig. S7: Variation of distance between the N3 atoms of paired bases along the MD simulated trajectory of 3’E (a) and 5’E-form (b) structure in deprotonated state with normal cytosine considering larger simulation box, and considering TIP3P water model in case of 5’E-form structure (c).

Fig. S8: 1^{st} and 2^{nd} normal mode of motions in the equilibrated MD trajectory of (a)-(b) 3’E and (c)-(d) 5’E-form structure under neutral pH with deprotonated cytosines.

Fig. S9: Average structure of i-motif core in the equilibrated MD trajectory of (a) 3’E and (b) 5’E-form topology under acidic pH with hemi-protonted cytosines.

Fig. S10: Average values along with standard deviations of narrow grooves and wide grooves backbone phosphate-phosphate distances in (a)-(b) 3’E and (c)-(d) 5’E-form i-motif structure under acidic pH with hemi-protonted cytosines.

Fig. S11: Variation of energy of the sugar-phosphate backbone refined conformation of model (a) $C^+C^+C^+$/CCC trinucleotide structure with helical rotations (θ) of the intercalated base pair around their base pair helix axis, and (b) tetranucleotide conformations of two intercalated C^+C^+/CC dinuceotides with helical rotations (θ) around their base pair helix axis.

Fig. S12: Radial distributions of the oxygen (O) atom of solvent water molecule around backbone phosphate group of bases ($g(r_{P-O})$) within i-motif core with hemi-protonated cytosines under acidic pH for (a) 3'E and (b) 5'E-form structure, and in deprotonated state of cytosines under neutral pH for (c) 3'E and (d) 5'E-form structure.

Fig. S13: Radial distributions of the oxygen (O) atoms of solvent water molecule around N4 atom of cytosines ($g(r)$) within i-motif core in hemi-protonated and deprotonated state of cytosines for (a) 3'E and (b) 5'E-form structure considering SPC/E water model, and (c) 5'E-form structure considering TIP3P water model.

Fig. S14: Radial distributions of the oxygen (O) atoms of solvent water molecule around N4 atom of cytosines ($g(r_{N4-O})$) within i-motif core at elevated temperatures with hemi-protonated cytosines under acidic pH for (a) 3'E and (b) 5'E-form i-motif structure.

Fig. S15: (a) DFT optimized geometry of six water molecules in wider grooves first solvation cell considering MD average model conformation of $C^+C^+C^+$/CCC trinucleotide within the i-motif core and fixing all the non-hydrogen atoms of the bases. (b) DFT optimized structure of a water molecule along with cytosine base.

Fig. S16: First normal mode of motions at different temperature in the equilibrated MD trajectory of (a)-(c) 3'E and (d)-(f) 5'E-form i-motif structure under acidic pH with hemi-protonated cytosines.

Fig. S17: Root mean square fluctuation (RMSF) of the nucleotides at different temperature in (a) 3'E and (b) 5'E-form i-motif structure with hemi-protonated cytosines under acidic pH.

Fig. S18: At different temperature distribution of wide grooves width in (a) 3'E and (b) 5'E-form structure, narrow grooves width in (c) 3'E and (d) 5'E-form structure, and hydrogen bonding distance and angle between sugar oxygen O4' of one strand and C1' on the anti-parallel strand across the narrow grooves in (e) 3'E and (f) 5'E-form structure, as derived from the equilibrated

MD trajectory of i-motif DNA under acidic pH with hemi-protonated cytosines.

Fig. S19: Temperature dependent grid water density distribution (ρ_{wat}) around the i-motif core in (a)-(c) 3'E and (d)-(f) 5'E-form structure under acidic pH having probability of water molecules stay in that grid points greater than 0.5. Grid points are represented with a sphere of color tints wheat.

Fig. S20: (a) At different temperature distribution of number of water molecules forming hydrogen bonds with the N4 atom of cytosines in the wide grooves of 5'E-form i-motif DNA in equilibrated trajectory under acidic pH. (b) Distribution of hydrogen bonded life time at different temperature for the hydrogen bonded water molecules in the wide grooves of 5'E-form structure with hemi-protonated cytosines.

Fig. S21: In case of 5'E_{CGG} (a)-(b) and 5'E_{GCC} (c)-(d) form structure first two normal modes of motions in the equilibrated trajectory. Distribution of (e) narrow grooves width and (f) hydrogen bonding distance and angle between sugar oxygen O4' of one strand and C1' on the anti-parallel strand across the narrow minor grooves in 5'E (TAA), 5'E_{CGG} (CGG) and 5'E_{GCC} (GCC) form structure, as derived from the equilibrated MD trajectory of i-motif DNA under acidic pH with hemi-protonted cytosines.

Tables:

Table S1: Base pair orientational parameters in model $C^+C^+C^+/CCC$ trinucleotide structure (ABC/DEF) as derived from the NMR structure of i-motif DNA (PDB id: 1EL2).

System	Base pair step parameters						
	Base pair step	Shift (Å)	Slide (Å)	Rise (Å)	Tilt (°)	Roll (°)	Twist (°)
ABC/DEF ($C^+C^+C^+/CCC$) trinucleotide conformation	AB/EF (A:F :: B:E)	-0.89	0.47	3.37	1.34	1.49	93.97
	BC/DE (B:E :: C:D)	0.17	0.72	2.81	6.37	0.10	106.89
	Base pair parameters						
	Base pair	Shear (Å)	Stagger (Å)	Stretch (Å)	Buckle (°)	Open (°)	Propeller (°)
	A:F	-0.13	-0.42	2.76	-6.78	-0.11	-0.64
	B:E	-0.55	-0.12	2.75	-12.79	0.85	1.08
	C:D	0.69	0.06	2.73	-7.25	-0.47	3.13

Table S2: Configurational entropy of the core and loop regions of the i-motif in 3'E and 5'E-form structure with hemi-protonated cytosines, derived from the normal mode analysis of equilibrated MD simulated trajectory at 300K.

System	Structural region	Configurational Entropy (cal/mol-K)
3'E-form structure (3'E topology)	Core	690.68
	Loop1	378.08
	Loop2	415.92
	Loop3	368.56
5'E-form structure (5'E topology)	Core	607.20
	Loop1	368.04
	Loop2	352.06
	Loop3	353.23

Table S3: Average value along with standard deviation of the base pair parameters as found in experimental dataset and MD simulation of 3’E and 5’E-form structure under acidic pH with hemi-protonated cytosines having two different topologies.

System	Base pair	Shear (Å)	Stagger (Å)	Stretch (Å)	Buckle (°)	Open (°)	Propeller (°)
Experimental Dataset	$C:C^+$	-0.33 [0.60]	0.07 [0.35]	2.62 [0.20]	0.95 [8.79]	0.83 [2.97]	0.86 [8.80]
3’E-form structure (3'E topology)	$C1:C^+12$	-0.22 [0.35]	-0.18 [0.44]	2.88 [0.12]	13.19 [9.78]	-3.44 [4.11]	-4.49 [7.33]
	$C2:C^+13$	-0.58 [0.25]	0.05 [0.29]	2.80 [0.09]	5.37 [9.12]	-2.09 [3.16]	2.82 [5.85]
	$C6:C^+17$	-0.57 [0.25]	0.09 [0.29]	2.81 [0.09]	13.11 [8.75]	-2.71 [3.06]	3.42 [5.43]
	$C7:C^+18$	-0.35 [0.25]	0.06 [0.30]	2.85 [0.08]	11.67 [8.63]	-2.86 [2.95]	-3.21 [6.05]
	T5:T16	-2.06 [0.43]	0.27 [0.55]	2.95 [0.18]	-16.41 [10.18]	-0.62 [7.11]	15.64 [9.94]
5’E-form structure (5'E topology)	$C1:C^+13$	-0.45 [0.27]	0.02 [0.31]	2.82 [0.09]	-3.82 [8.34]	-2.41 [3.28]	6.10 [6.47]
	$C2:C^+14$	-0.56 [0.25]	0.02 [0.29]	2.80 [0.08]	10.33 [8.29	-1.87 [2.96]	2.72 [5.69]
	$C3:C^+15$	-0.36 [0.29]	0.05 [0.31]	2.84 [0.09]	15.77 [9.12]	-2.50 [3.06]	-0.77 [6.78]
	$C7^+:C19$	-0.18 [0.31]	0.05 [0.36]	2.86 [0.09]	-12.15 [14.11]	2.67 [3.43]	7.71 [9.49]
	$C8^+:C20$	-0.70 [0.24]	0.05 [0.27]	2.78 [0.09]	3.77 [8.73]	2.71 [3.23]	0.93 [5.82]
	$C9^+:C21$	-0.52 [0.25]	-0.01 [0.29]	2.83 [0.09]	14.15 [8.19]	2.66 [3.14]	-1.68 [5.47]
	T10:T22	2.47 [0.28]	0.00 [0.42]	2.84 [0.12]	20.19 [8.85]	-1.40 [5.61]	-16.57 [7.45]

Table S4: Average value along with standard deviation of the backbone dihedral angles for the bases as found in MD simulation of 5'E-form i-motif structure under acidic pH with hemi-protonated cytosines.

Nucleotide	α (°)	β (°)	γ (°)	δ (°)	ε (°)	ζ (°)	χ (°)	Phase (°)
C1	0.00 [0.0]	0.00 [0.0]	65.50 [22.5]	88.79 [21.4]	200.27 [19.1]	275.07 [9.9]	-127.60 [10.7]	51.68 [41.6]
C2	293.27 [15.8]	174.64 [21.5]	73.19 [27.2]	86.59 [10.3]	192.10 [10.4]	277.85 [8.2]	-127.94 [8.4]	35.64 [27.2]
C3	293.31 [26.0]	176.78 [10.6]	71.73 [23.3]	94.08 [19.5]	214.75 [15.4]	294.15 [10.4]	-125.34 [13.2]	53.57 [43.6]
T4	276.27 [27.1]	220.08 [36.7]	301.10 [14.1]	142.80 [12.6]	188.65 [9.5]	277.37 [9.2]	-114.40 [14.7]	154.97 [16.6]
A5	288.72 [9.7]	171.07 [8.7]	55.65 [9.7]	136.17 [12.1]	230.14 [17.2]	289.39 [25.5]	-99.12 [14.5]	145.52 [19.8]
A6	190.18 [66.9]	180.24 [11.6]	58.34 [13.4]	150.02 [9.3]	209.52 [19.2]	280.66 [10.5]	-132.61 [26.8]	177.43 [23.3]
C^+7	294.27 [9.36]	182.68 [12.4]	66.40 [9.5]	86.06 [8.6]	190.20 [11.6]	272.54 [11.9]	-124.71 [14.5]	24.34 [13.2]
C^+8	295.76 [10.6]	181.26 [10.6]	68.52 [9.3]	100.41 [20.8]	188.32 [8.9]	275.30 [10.7]	-121.21 [11.0]	46.06 [45.3]
C^+9	292.61 [28.6]	180.31 [10.2]	76.32 [18.8]	125.24 [21.8]	195.91 [14.4]	253.92 [24.4]	-111.04 [13.7]	122.74 [40.7]
T10	290.17 [11.9]	184.19 [22.4]	56.88 [10.8]	137.96 [10.0]	193.81 [14.6]	271.52 [20.5]	-96.76 [14.0]	149.41 [15.1]
A11	280.32 [13.5]	69.59 [9.49]	179.67 [8.2]	146.36 [11.7]	243.07 [28.4]	168.20 [11.4]	-133.02 [23.5]	158.36 [18.0]
A12	75.59 [15.8]	182.29 [24.1]	60.11 [13.1]	148.06 [9.1]	228.80 [34.0]	70.33 [34.2]	-121.14 [22.4]	167.81 [18.8]
C^+13	269.83 [17.9]	168.71 [30.3]	61.10 [13.7]	96.81 [21.5]	209.87 [25.1]	272.57 [14.4]	-138.58 [11.4]	64.07 [38.3]
C^+14	292.28 [21.3]	173.53 [30.3]	72.02 [18.0]	130.66 [19.6]	198.58 [15.1]	260.62 [23.6]	-108.23 [16.2]	135.25 [31.0]
C^+15	276.40 [24.8]	181.50 [17.5]	69.62 [34.7]	109.65 [19.8]	236.59 [27.9]	273.22 [18.4]	-106.18 [14.4]	103.76 [34.1]
T16	237.20 [46.4]	193.16 [32.3]	60.26 [14.91]	145.69 [7.9]	199.96 [9.86]	282.87 [10.8]	-130.09 [14.6]	163.42 [13.7]
A17	277.24 [12.0]	172.33 [8.9]	48.86 [12.8]	136.15 [10.7]	223.42 [20.31]	289.68 [9.8]	-92.19 [15.4]	146.04 [15.9]
A18	262.73 [41.4]	173.27 [18.0]	81.32 [25.4]	156.09 [7.3]	214.10 [30.0]	164.33 [21.8]	-94.10 [25.2]	179.20 [13.5]
C19	224.15 [29.8]	177.66 [16.0]	69.53 [38.6]	104.92 [24.1]	203.87 [12.6]	280.29 [9.9]	-117.05 [11.0]	38.22 [51.9]
C20	287.79 [27.6]	172.51 [18.1]	86.28 [30.8]	83.23 [9.6]	190.37 [10.5]	276.32 [8.6]	-126.45 [9.3]	39.80 [24.8]
C21	295.25 [20.1]	177.06 [8.42]	69.24 [16.15]	82.31 [8.0]	197.30 [18.5]	278.44 [10.5]	-127.35 [8.6]	38.64 [19.8]
T22	289.40 [21.5]	152.57 [45.7]	88.33 [33.2]	120.28 [40.0]	0.00 [0.0]	0.00 [0.0]	-122.07 [15.8]	108.77 [46.8]

Table S5: Average value along with standard deviation of the backbone dihedral angles for the bases as found in MD simulation of 3'E-form i-motif structure under acidic pH with hemi-protonated cytosines.

Nucleotide	α (°)	β (°)	γ (°)	δ (°)	ε (°)	ζ (°)	χ (°)	Phase (°)
C1	0.00 [0.0]	0.00 [0.0]	65.09 [25.4]	124.92 [21.0]	235.57 [23.2]	288.78 [11.6]	-129.75 [11.7]	137.75 [22.5]
C2	231.57 [50.3]	110.39 [52.3]	188.77 [10.8]	119.18 [21.6]	227.06 [25.9]	268.75 [21.9]	-127.23 [14.2]	135.11 [14.8]
T3	76.43 [27.0]	159.50 [20.7]	62.43 [17.3]	147.46 [7.1]	236.96 [36.5]	284.11 [12.5]	-128.42 [16.9]	165.00 [11.8]
T4	94.94 [39.0]	175.01 [13.7]	300.14 [12.0]	150.13 [9.1]	266.45 [24.2]	71.59 [26.0]	-128.53 [14.8]	163.81 [13.9]
T5	246.77 [14.5]	168.95 [14.4]	55.35 [9.5]	94.51 [14.7]	186.82 [9.1]	276.13 [8.2]	-107.45 [9.9]	2.97 [21.8]
C6	300.37 [9.1]	173.03 [8.8]	65.10 [8.4]	84.94 [7.7]	193.94 [8.9]	279.25 [8.2]	-131.57 [7.9]	26.84 [17.9]
C7	301.01 [9.6]	180.15 [10.3]	72.17 [10.4]	88.59 [7.2]	202.71 [17.8]	287.51 [12.6]	-120.42 [15.2]	34.61 [14.9]
T8	291.39 [9.5]	175.0 [10.2]	62.25 [9.9]	141.51 [9.9]	211.02 [29.4]	255.65 [30.8]	-116.73 [17.6]	156.40 [16.7]
T9	122.35 [31.9]	184.18 [21.5]	56.49 [12.6]	146.84 [8.6]	201.78 [11.8]	285.70 [8.7]	-137.67 [16.9]	161.70 [13.5]
T10	279.48 [11.0]	174.19 [11.3]	46.60 [17.7]	127.15 [18.2]	187.85 [11.2]	274.81 [10.5]	-109.24 [16.5]	135.49 [27.6]
A11	285.95 [10.9]	171.38 [9.7]	54.08 [8.8]	104.06 [26.8]	195.83 [11.2]	275.77 [10.4]	-121.30 [14.5]	85.32 [35.2]
C^+12	298.31 [10.4]	180.33 [9.9]	66.73 [10.3]	115.58 [24.4]	193.94 [13.1]	261.79 [19.5]	-116.53 [15.6]	101.53 [38.5]
C^+13	297.38 [15.3]	182.67 [11.7]	56.49 [12.6]	126.90 [17.3]	214.86 [30.2]	222.81 [28.8]	-106.94 [11.5]	131.48 [32.4]
T14	59.28 [14.3]	172.06 [18.3]	289.35 [17.4]	147.60 [11.2]	213.24 [18.5]	172.73 [15.1]	62.92 [12.3]	158.90 [15.0]
T15	68.28 [13.1]	200.86 [21.0]	55.57 [10.2]	136.71 [11.0]	219.95 [24.8]	45.73 [13.7]	-126.65 [21.8]	151.39 [20.2]
T16	74.60 [11.9]	179.60 [14.5]	301.43 [9.1]	83.05 [12.0]	188.78 [10.0]	269.89 [8.8]	-129.73 [9.5]	38.06 [24.5]
C^+17	304.72 [10.3]	180.11 [9.4]	73.49 [9.2]	135.09 [20.6]	195.11 [14.4]	256.00 [21.2]	-110.25 [13.5]	164.42 [24.5]
C^+18	289.52 [24.3]	181.62 [23.5]	66.92 [29.6]	129.90 [18.1]	0.00 [0.0]	0.00 [0.0]	-102.23 [15.4]	136.48 [27.1]

Table S6: Average value along with standard deviation of the base pair parameters as found in MD simulation of 5’E-form structure in deprotonated state with normal cytosines.

System	Base pair	Shear (Å)	Stagger (Å)	Stretch (Å)	Buckle (°)	Open (°)	Propeller (°)
5’E-form structure with normal cytosine	C1:C13	6.50 [1.5]	-1.47 [1.9]	3.92 [2.3]	-55.86 [15.7]	-30.62 [19.3]	12.66 [15.5]
	C2:C14	1.99 [2.4]	-0.35 [1.8]	3.70 [1.2]	17.30 [37.2]	30.90 [24.5]	40.21 [20.0]
	C3:C15	2.46 [0.4]	2.40 [0.7]	2.88 [0.7]	53.26 [14.0]	-40.98 [10.3]	74.92 [9.0]
	C7:C19	-2.35 [0.8]	6.13 [0.7]	5.44 [0.7]	-31.45 [11.8]	-13.84 [8.3]	-30.43 [8.1]
	C8:C20	-2.47 [1.1]	9.25 [1.0]	1.52 [1.3]	36.62 [20.6]	48.27 [10.9]	2.95 [13.5]
	C9:C21	0.26 [1.4]	0.78 [1.7]	3.13 [0.9]	47.57 [30.8]	17.88 [25.5]	67.98 [44.1]

Table S7: Average value along with standard deviation of the backbone dihedral angles for the bases as found in MD simulation of 5'E-form structure in deprotonated state with normal cytosines.

Nucleotide	α (°)	β (°)	γ (°)	δ (°)	ε (°)	ζ (°)	χ (°)	Phase (°)
C1	0.00 [0.0]	0.00 [0.0]	63.69 [19.4]	79.84 [7.3]	211.00 [17.3]	277.02 [12.1]	-133.11 [15.0]	29.72 [15.2]
C2	290.06 [13.0]	192.02 [9.9]	59.17 [11.1]	85.88 [9.1]	225.28 [11.8]	294.27 [9.3]	-131.08 [16.4]	53.46 [18.3]
C3	296.83 [10.0]	196.61 [9.8]	63.57 [9.9]	139.20 [7.8]	233.00 [14.1]	280.10 [12.1]	-71.12 [7.6]	146.80 [10.9]
T4	94.13 [20.2]	184.43 [12.4]	62.38 [8.9]	143.84 [7.0]	193.17 [7.9]	278.78 [6.9]	-121.52 [12.4]	159.68 [11.8]
A5	292.94 [8.1]	169.94 [8.3]	54.00 [7.6]	141.97 [7.0]	222.32 [11.3]	293.27 [9.7]	-90.40 [13.1]	152.10 [10.7]
A6	184.86 [18.4]	183.22 [11.1]	57.45 [13.9]	148.53 [6.8]	193.86 [8.3]	274.02 [7.6]	-156.84 [11.6]	191.30 [14.5]
C7	291.57 [9.3]	172.95 [8.8]	57.89 [7.9]	82.43 [6.6]	216.61 [11.5]	283.14 [8.4]	-135.63 [9.2]	21.18 [11.4]
C8	295.29 [15.7]	193.91 [14.2]	59.25 [11.4]	84.01 [17.5]	196.14 [13.7]	268.37 [20.7]	-94.58 [11.8]	62.35 [27.8]
C9	284.37 [14.8]	185.57 [10.4]	55.06 [9.1]	84.63 [7.7]	218.23 [15.6]	281.98 [20.9]	-132.35 [14.5]	24.25 [12.4]
T10	89.53 [9.8]	185.03 [29.2]	291.47 [8.7]	135.13 [11.3]	227.87 [21.1]	161.25 [13.8]	-119.65 [17.3]	146.62 [17.2]
A11	81.90 [17.1]	182.79 [15.1]	62.13 [10.9]	141.67 [11.8]	201.09 [14.0]	274.19 [17.0]	140.93 [19.8]	155.45 [26.5]
A12	197.76 [17.5]	168.74 [13.6]	61.38 [10.7]	151.05 [6.4]	223.60 [11.4]	288.20 [8.6]	-145.67 [21.5]	178.26 [13.7]
C13	288.96 [9.0]	174.60 [9.1]	59.74 [7.3]	144.02 [8.9]	232.71 [17.4]	288.64 [9.9]	-129.29 [13.6]	163.73 [19.9]
C14	279.43 [13.4]	177.84 [10.7]	53.58 [10.3]	140.60 [8.2]	209.13 [23.3]	216.95 [57.4]	-121.94 [26.4]	159.64 [14.8]
C15	279.38 [22.8]	221.30 [40.4]	55.43 [12.0]	147.24 [10.2]	232.72 [15.4]	294.03 [12.0]	-140.38 [16.2]	159.27 [15.2]
T16	236.44 [60.7]	184.11 [13.9]	53.52 [11.3]	145.98 [8.6]	200.98 [11.8]	283.64 [7.7]	-132.40 [14.8]	160.93 [13.5]
A17	282.86 [10.8]	169.85 [8.2]	46.28 [9.4]	141.74 [8.9]	231.10 [24.1]	188.81 [23.9]	-92.06 [14.2]	148.46 [11.0]
A18	286.44 [12.3]	152.39 [15.3]	52.95 [10.5]	142.96 [9.2]	185.88 [9.5]	270.83 [8.6]	-112.60 [11.9]	170.30 [21.7]
C19	291.24 [10.0]	168.87 [8.5]	57.39 [8.6]	131.14 [14.9]	219.56 [10.6]	288.42 [9.3]	-107.65 [12.0]	136.21 [22.8]
C20	285.97 [10.5]	172.68 [10.1]	59.71 [8.2]	145.59 [8.7]	210.28 [23.5]	162.90 [10.8]	-112.82 [17.4]	166.53 [17.5]
C21	257.27 [36.0]	162.32 [18.1]	50.0 [11.0]	143.13 [11.9]	219.45 [24.9]	152.12 [15.8]	-136.73 [17.0]	162.91 [24.6]
T22	235.44 [85.2]	182.70 [17.7]	60.03 [11.0]	146.33 [11.7]	0.00 [0.0]	0.00 [0.0]	-135.94 [20.6]	168.70 [23.6]

Table S8: Average hydrogen bonding geometry and occupancy (considering C – O distance ≤ 3.4 Å and C-H...O angle > 120°) of possible C-H...O mediated hydrogen bond between sugar moieties of the antiparallel strands along the narrow grooves of i-motif DNA.

Structure	C-H...O mediated hydrogen bond between sugar moiety	Distance between C and O (Å)	C-H...O angle (°)	Occupancy (%)
5'E i-motif	(C1) C1'-H...O4' (T22)	3.30	138.03	51.33
	(T22) C1'-H...O4' (C1)	3.32	137.86	32.24
	(C2) C1'-H...O4' (C21)	3.27	132.14	71.00
	(C21) C1'-H...O4' (C2)	3.26	131.71	72.11
	(C3) C1'-H...O4' (C20)	3.29	131.07	55.74
	(C20) C1'-H...O4' (C3)	3.25	131.16	70.29
	(C^+8) C1'-H...O4' (C^+15)	3.29	136.34	65.10
	(C^+15) C1'-H...O4' (C^+8)	3.36	131.12	18.31
	(C^+9) C1'-H...O4' (C^+14)	3.29	131.14	47.22
	(C^+14) C1'-H...O4' (C^+9)	3.30	130.74	43.15
	(T10) C1'-H...O4' (C^+13)	3.38	126.16	10.0
	(C^+13) C1'-H...O4' (T10)	3.30	149.18	82.10
3'E i-motif	(C1) C1'-H…O4'(C7)	3.27	134.46	56.75
	(C7) C1'-H…O4'(C1)	3.31	130.51	17.70
	(C2) C1'-H…O4'(C6)	3.29	135.51	64.64
	(C6) C1'-H…O4'(C2)	3.28	133.41	67.24
	(C^+12) C1'-H…O4'(C^+18)	3.30	139.27	51.27
	(C^+18) C1'-H…O4'(C^+12)	3.32	134.16	23.59
	(C^+13) C1'-H…O4'(C^+17)	3.29	133.26	54.27
	(C^+17) C1'-H…O4'(C^+13)	3.31	131.11	37.35

Table S9: Base pairing and stacking energy between the stacked base pairs in model $C^+C^+C^+/CCC$ trinucleotide structure (ABC/DEF) as derived from the NMR structure of i-motif DNA (PDB id: 1EL2).

System	Quantum chemical method	Base pairing energy (kcal/mol)			Stacking energy between consecutive base pairs (kcal/mol)		Stacking energy between the stacked base pairs in trinucleotide step [ABC/DEF – (A:F + B:E + C:D)] (kcal/mol)
		A:F	B:E	C:D	AB/EF	BC/DE	
Partial optimized geometry of $C^+C^+C^+/CCC$ trinucleotide structure	ωB97X-D/cc-pVDZ	-55.51	-54.50	-50.31	28.93	27.77	91.18
	B3LYP-D3/cc-pVDZ	-57.06	-55.97	-51.49	26.64	25.80	87.09
	MO6-2X/cc-pVDZ	-53.92	-53.86	-49.53	28.16	28.22	90.75
Full optimized geometry of $C^+C^+C^+/CCC$ trinucleotide structure	ωB97X-D/cc-pVDZ	-57.59	-59.01	-58.04	20.77	17.64	70.56
	B3LYP-D3/cc-pVDZ	-56.09	-57.50	-56.57	22.48	21.74	75.02
	MO6-2X/cc-pVDZ	-54.62	-55.96	-54.98	22.09	20.94	73.91
Full optimized geometry of CCC/CCC trinucleotide structure	ωB97X-D/cc-pVDZ	-28.80	-28.48	-28.06	-24.66	-34.72	-61.04
	B3LYP-D3/cc-pVDZ	-27.74	-27.43	-27.04	-21.82	-30.17	-53.49
	MO6-2X/cc-pVDZ	-26.42	-26.17	-25.80	-23.83	-31.55	-56.71

Table S10: Variation of stacking energy between the stacked base pairs in model $C^+C^+C^+$/CCC trinucleotide structure (ABC/DEF) with stacking interval between the consecutive base pairs.

Stacking interval between consecutive base pairs (Å)	ωB97X-D/cc-pVDZ Stacking energy between consecutive base pairs (kcal/mol)		ωB97X-D/cc-pVDZ Stacking energy between the stacked base pairs in trinucleotide step (kcal/mol)	B3LYP-D3/cc-pVDZ Stacking energy between consecutive base pairs (kcal/mol)		B3LYP-D3/cc-pVDZ Stacking energy between the stacked base pairs in trinucleotide step (kcal/mol)	MO6-2X/cc-pVDZ Stacking energy between consecutive base pairs (kcal/mol)		MO6-2X/cc-pVDZ Stacking energy between the stacked base pairs in trinucleotide step (kcal/mol)
	AB/EF	BC/DE		AB/EF	BC/DE		AB/EF	BC/DE	
(1.98, 4.20)	868.255	38.606	941.101	865.115	37.606	937.884	861.514	39.372	934.973
(2.18, 4.00)	496.518	38.453	569.747	493.990	37.993	566.989	486.713	39.219	560.861
(2.38, 3.80)	291.921	36.538	363.848	289.163	35.849	360.630	281.197	37.840	354.349
(2.58, 3.60)	166.604	34.546	236.999	163.923	33.474	233.628	156.799	36.308	228.879
(2.78, 3.40)	93.988	32.248	162.391	91.613	31.099	159.021	85.945	34.010	156.263
(2.98, 3.20)	55.918	30.257	122.100	53.237	28.495	118.116	49.943	31.789	118.270
(3.18, 3.00)	37.074	27.959	101.265	34.546	26.044	97.128	34.087	29.414	99.733
(3.38, 2.80)	29.49	26.886	92.685	27.116	24.742	88.396	28.342	26.886	91.919
(3.58, 2.60)	27.346	29.108	92.839	25.201	26.657	88.549	27.806	27.576	92.073
(3.78, 2.40)	27.959	37.917	102.337	26.274	35.466	98.201	29.338	34.163	100.039
(3.98, 2.20)	29.644	59.211	125.164	28.265	56.530	121.180	31.406	52.624	120.414
(4.18, 2.00)	31.482	101.877	169.591	30.333	99.196	165.914	33.091	92.915	162.391
(4.38, 1.80)	33.397	180.315	249.561	32.478	177.941	246.497	34.700	169.898	240.522
(4.58, 1.60)	34.929	315.207	385.755	34.546	314.594	384.836	36.078	304.943	376.410
(4.78, 1.40)	35.849	537.345	608.813	35.849	540.409	611.724	36.921	527.694	600.080

Table S11: Average hydrogen bonding geometry and occupancy (considering C – O distance ≤ 3.4 Å and C-H...O angle > 120°) of possible C-H...O mediated hydrogen bond between sugar moieties of the antiparallel strands along the narrow grooves of i-motif DNA at elevated temperatures.

C-H...O mediated hydrogen bond between sugar moiety	320K			340K		
	Distance between C and O (Å)	C-H...O angle (°)	Occupancy (%)	Distance between C and O (Å)	C-H...O angle (°)	Occupancy (%)
5’E i-motif						
(C1) C1'-H...O4' (T22)	3.29	136.72	42.21	3.31	137.44	14.41
(T22) C1'-H...O4' (C1)	3.32	139.89	30.51	3.32	139.76	10.27
(C2) C1'-H...O4' (C21)	3.26	131.68	68.21	3.26	132.98	69.01
(C21) C1'-H...O4' (C2)	3.26	131.10	66.51	3.27	131.76	60.13
(C3) C1'-H...O4' (C20)	3.30	129.49	40.40	3.29	130.16	42.93
(C20) C1'-H...O4' (C3)	3.25	130.55	64.22	3.25	131.10	63.16
(C^+8) C1'-H...O4' (C^+15)	3.29	134.92	56.72	3.29	134.43	56.15
(C^+15) C1'-H...O4' (C^+8)	3.34	130.00	10.82	3.33	129.85	12.40
(C^+9) C1'-H...O4' (C^+14)	3.29	131.52	43.10	3.29	131.45	31.57
(C^+14) C1'-H...O4' (C^+9)	3.30	133.58	38.51	3.30	134.83	44.39
(T10) C1'-H...O4' (C^+13)	3.35	131.72	1.90	3.35	131.78	18.46
(C^+13) C1'-H...O4' (T10)	3.28	141.63	66.12	3.28	134.52	40.93
3’E i-motif						
(C1) C1’-H…O4’(C7)	3.23	130.04	52.25	3.24	135.30	65.52
(C7) C1’-H…O4’(C1)	3.34	128.42	2.6	3.33	128.31	1.31
(C2) C1’-H…O4’(C6)	3.34	136.84	2.50	3.35	132.10	6.36
(C6) C1’-H…O4’(C2)	3.28	142.69	54.44	3.26	137.69	64.15
(C^+12) C1’-H…O4’(C^+18)	3.29	140.66	62.18	3.25	132.88	57.59
(C^+18) C1’-H…O4’(C^+12)	3.37	131.88	2.31	3.33	130.74	3.39
(C^+13) C1’-H…O4’(C^+17)	3.32	129.03	19.63	3.30	130.81	1.48
(C^+17) C1’-H…O4’(C^+13)	3.27	138.40	61.20	3.30	150.97	61.18

Table S12: Average value along with standard deviation of the base pair step parameters as found in MD simulation of 5'E_{GCC} and 5'E_{CGG} form structure (':' denotes base pair and '::' denotes base pairs stack).

System	Base pair step	Shift (Å)	Slide (Å)	Rise (Å)	Tilt (°)	Roll (°)	Twist (°)
5'E_{GCC}-form structure (5'E topology)	CC/C^+C^+ (1:13 :: 2:14)	0.33 [0.44]	0.16 [0.42]	6.19 [0.23]	1.33 [3.11]	-1.01 [4.18]	18.13 [4.02]
	CC/C^+C^+ (2:14 :: 3:15)	0.50 [0.47]	0.20 [0.45]	6.34 [0.24]	1.04 [3.93]	-1.64 [3.56]	16.61 [4.98]
	C^+C^+/CC (7:19 :: 8:20)	-0.57 [0.43]	-0.84 [0.39]	6.04 [0.20]	3.04 2.77]	-2.28 [4.39]	17.28 [3.24]
	C^+C^+/CC (8:20 :: 9:21)	-0.34 [0.47]	-0.25 [0.44]	6.31 [0.24]	0.14 [3.71]	-1.26 [3.81]	17.90 [4.31]
5'E_{CGG}-form structure (5'E topology)	CC/C^+C^+ (1:13 :: 2:14)	0.26 [0.41]	0.03 [0.40]	6.13 [0.21]	0.64 [3.14]	-0.93 [3.82]	19.63 [3.79]
	CC/C^+C^+ (2:14 :: 3:15)	0.28 [0.43]	0.16 [0.36]	6.39 [0.24]	-0.06 [3.58]	0.17 [3.51]	19.10 [3.92]
	C^+C^+/CC (7:19 :: 8:20)	-0.23 [0.40]	-0.27 [0.37]	6.13 [0.21]	2.80 [2.93]	-3.38 [4.04]	14.98 [3.01]
	C^+C^+/CC (8:20 :: 9:21)	-0.26 [0.44]	-0.04 [0.35]	6.19 [0.21]	-0.45 [3.14]	-0.26 [3.56]	18.73 [3.49]

Table S13: Average value along with standard deviation of stacking interval and twist between consecutive stacked base pair within i-motif core as found in MD simulation of 5’E_{GCC} and 5’E_{CGG}-form structure (‘:’ denotes base pair and ‘::’ denotes base pairs stack).

System	Base pair step	Stacking interval (Å)	Twist between consecutive stacked base pair (°)
5’E_{GCC}-form structure (5'E topology)	CC^+/CC^+ (1:13 :: 9:21)	3.44 [0.24]	113.80 [3.94]
	CC^+/CC^+ (21:9 :: 14:2)	2.74 [0.22]	84.25 [3.06]
	CC^+/CC^+ (2:14 :: 8:20)	3.56 [0.23]	113.64 [5.09]
	CC^+/CC^+ (20:8 :: 15:3)	2.77 [0.23]	82.98 [3.74]
	CC^+/CC^+ (3:15 :: 7:19)	3.24 [0.26]	114.16 [4.42]
5’E_{CGG}-form structure (5'E topology)	CC^+/CC^+ (1:13 :: 9:21)	3.40 [0.24]	114.10 [4.44]
	CC^+/CC^+ (21:9 :: 14:2)	2.72 [0.24]	85.48 [2.95]
	CC^+/CC^+ (2:14 :: 8:20)	3.45 [0.24]	113.23 [4.21]
	CC^+/CC^+ (20:8 :: 15:3)	2.93 [0.24]	85.88 [2.89]
	CC^+/CC^+ (3:15 :: 7:19)	3.18 [0.25]	108.98 [3.39]

Table S14: Average value along with standard deviation of the backbone dihedral angles for the bases as found in MD simulation of 5'E_{GCC}-form structure.

Nucleotide	α (°)	β (°)	γ (°)	δ (°)	ε (°)	ζ (°)	χ (°)	Phase (°)
C1	0.00 [0.0]	0.00 [0.0]	66.0 [26.2]	95.53 [25.1]	213.31 [23.9]	279.34 [11.1]	-133.15 [14.0]	70.10 [49.1]
C2	288.98 [22.5]	189.75 [9.8]	80.98 [18.3]	90.15 [17.2]	193.67 [14.9]	279.83 [9.7]	-124.17 [10.8]	57.91 [38.3]
C3	281.07 [38.1]	173.10 [23.8]	89.2 [36.0]	112.06 [26.4]	231.27 [19.0]	289.54 [11.3]	-116.30 [11.8]	106.49 [43.3]
G4	143.68 [834.2]	180.69 [16.8]	63.52 [32.6]	147.14 [9.3]	188.56 [15.9]	262.69 [17.5]	-129.41 [20.6]	167.20 [15.3]
C5	288.31 [10.8]	188.98 [14.8]	50.48 [11.6]	139.51 [8.6]	250.08 [18.7]	278.24 [12.1]	-130.11 [17.6]	155.67 [15.7]
C6	216.32 [38.7]	168.62 [21.4]	56.26 [12.6]	145.97 [7.9]	210.65 [16.1]	283.23 [10.0]	-128.23 [15.7]	164.96 [13.8]
$C^{+}7$	288.74 [9.8]	171.30 [10.2]	60.05 [7.6]	85.13 [9.0]	192.09 [11.3]	273.02 [10.8]	-143.12 [9.3]	37.97 [46.0]
$C^{+}8$	300.43 [10.6]	183.55 [10.6]	71.27 [9.5]	118.10 [26.6]	193.88 [11.6]	268.44 [17.6]	-120.63 [13.9]	110.45 [41.7]
$C^{+}9$	292.20 [24.2]	178.62 [16.1]	78.54 [31.7]	130.48 [16.8]	250.35 [34.7]	218.67 [31.7]	-106.51 [14.5]	138.43 [24.6]
G10	287.22 [12.1]	154.81 [24.3]	57.63 [10.7]	145.55 [7.7]	183.18 [11.9]	273.02 [9.6]	-103.73 [11.6]	167.30 [15.3]
C11	291.04 [13.6]	168.71 [11.2]	64.30 [9.3]	139.36 [13.8]	276.44 [20.9]	73.73 [14.7]	-126.13 [21.7]	148.58 [18.2]
C12	72.08 [11.8]	190.97 [15.5]	298.22 [8.9]	151.95 [8.8]	233.14 [32.0]	139.13 [24.2]	-147.31 [16.9]	172.33 [17.0]
$C^{+}13$	272.31 [22.9]	144.42 [24.5]	55.23 [9.4]	86.20 [7.9]	195.25 [9.6]	273.39 [8.9]	-136.18 [8.1]	42.89 [41.0]
$C^{+}14$	299.26 [13.1]	178.87 [10.0]	74.20 [12.6]	123.69 [26.3]	197.67 [13.8]	270.65 [14.7]	-115.23 [12.8]	131.54 [43.4]
$C^{+}15$	279.17 [28.8]	185.59 [21.0]	70.98 [31.7]	119.46 [19.8]	242.43 [30.2]	258.86 [29.8]	-99.55 [8.3]	122.05 [45.8]
G16	270.60 [34.4]	184.04 [16.5]	108.45 [49.1]	147.65 [14.2]	208.20 [14.0]	275.48 [15.2]	148.29 [15.6]	170.22 [27.6]
C17	206.75 [25.0]	169.13 [16.2]	59.24 [13.3]	149.73 [6.9]	229.73 [18.3]	291.35 [10.6]	-146.95 [21.3]	170.94 [14.11]
C18	288.89 [14.1]	169.66 [12.1]	69.09 [21.9]	145.76 [8.3]	225.13 [20.2]	177.02 [14.9]	-127.79 [14.8]	162.24 [14.7]
C19	201.42 [24.1]	188.35 [14.0]	63.22 [13.2]	95.56 [7.3]	201.39 [9.8]	279.21 [7.9]	-112.15 [8.8]	0.03 [20.2]
C20	294.94 [10.5]	174.20 [8.8]	67.09 [9.4]	85.50 [7.0]	190.84 [8.8]	279.05 [8.1]	-126.80 [7.9	24.11 [14.2]
C21	294.91 [21.8]	178.49 [8.6]	70.02 [15.3]	80.73 [7.9]	188.42 [14.5]	278.05 [10.9]	-124.87 [8.7]	33.13 [17.3]
G22	297.2 [12.7]	193.79 [11.0]	63.88 [15.9]	132.07 [19.8]	0.00 [0.0]	0.00 [0.0]	-110.18 [20.8]	111.31 [45.4]

Table S15: Average value along with standard deviation of the backbone dihedral angles for the bases as found in MD simulation of 5'E_{CGG}-form structure.

Nucleotide	α (°)	β (°)	γ (°)	δ (°)	ε (°)	ζ (°)	χ (°)	Phase (°)
C1	0.00 [0.0]	0.00 [0.0]	64.26 [18.5]	82.62 [12.9]	197.20 [14.7]	275.79 [9.2]	-128.75 [9.6]	39.71 [28.6]
C2	294.77 [21.8]	174.78 [15.8]	69.60 [20.0]	85.12 [9.0]	191.20 [9.5]	280.59 [8.3]	-126.83 [8.6]	33.74 [23.8]
C3	297.42 [18.2]	178.68 [8.9]	68.88 [13.8]	82.91 [11.7]	210.73 [22.8]	285.69 [11.1]	-121.63 [10.0]	45.47 [21.7]
C4	232.01 [41.5]	253.94 [46.1]	298.37 [10.9]	150.75 [10.7]	190.10 [8.1]	280.14 [8.3]	-110.09 [13.9]	166.21 [15.9]
G5	288.90 [8.8]	168.11 [8.0]	56.84 [8.1]	141.40 [7.5]	270.94 [10.9]	283.46 [13.8]	-88.16 [11.3]	152.07 [11.6]
G6	238.02 [47.0]	179.07 [12.5]	53.36 [11.9]	147.29 [9.3]	203.55 [13.9]	283.80 [9.9]	-119.82 [36.4]	164.22 [17.1]
C^+7	290.34 [11.2]	174.15 [10.3]	63.41 [10.1]	83.28 [7.9]	189.59 [11.2]	271.10 [10.9]	-132.81 [10.5]	28.53 [16.1]
C^+8	298.52 [9.8]	177.46 [10.1]	68.95 [8.5]	98.42 [19.5]	187.94 [9.8]	273.21 [12.1]	-124.53 [11.0]	19.53 [14.3]
C^+9	297.76 [16.3]	180.69 [9.4]	72.79 [15.5]	116.60 [25.4]	202.01 [22.0]	258.30 [29.7]	-113.96 [12.7]	96.93 [21.7]
C10	282.59 [30.2]	137.65 [41.7]	79.48 [39.8]	143.80 [11.6]	210.43 [32.8]	259.22 [32.7]	-113.55 [15.2]	158.37 [19.9]
G11	291.82 [13.0]	163.03 [16.7]	55.72 [9.7]	143.0 [11.9]	251.41 [29.3]	138.10 [38.1]	112.17 [34.6]	157.99 [19.5]
G12	281.47 [11.2]	70.77 [22.9]	186.41 [34.6]	144.81 [11.0]	221.09 [29.7]	155.29 [14.8]	-118.75 [29.7]	159.39 [20.0]
C^+13	285.71 [14.1]	173.13 [13.4]	59.02 [9.1]	102.27 [22.2]	203.54 [26.3]	274.87 [13.3]	-131.33 [12.6]	67.79 [34.0]
C^+14	294.22 [18.3]	188.67 [10.5]	78.17 [19.4]	132.75 [16.4]	199.11 [14.6]	260.67 [21.1]	-108.37 [15.6]	141.30 [31.5]
C^+15	287.32 [15.7]	185.91 [15.2]	66.33 [18.8]	124.36 [14.9]	249.00 [24.1]	267.61 [20.2]	-92.26 [12.9]	128.33 [16.8]
C16	107.07 [46.3]	179.38 [18.1]	57.29 [10.7]	145.56 [9.3]	220.74 [24.4]	283.61 [10.8]	-137.74 [21.5]	157.64 [12.4]
G17	264.64 [32.9]	242.09 [48.3]	299.86 [8.1]	139.77 [13.0]	186.76 [10.9]	276.50 [8.9]	67.24 [16.0]	150.44 [16.0]
G18	290.93 [8.8]	172.54 [8.8]	55.91 [8.3]	131.73 [11.0]	246.64 [13.8]	289.63 [9.5]	-95.42 [13.5]	142.04 [20.1]
C19	263.23 [19.2]	166.03 [14.1]	53.66 [11.4]	87.94 [8.0]	195.76 [11.1]	275.22 [8.2]	-114.10 [10.1]	17.66 [19.4]
C20	295.52 [9.7]	175.18 [9.0]	64.87 [8.2]	85.83 [7.5]	189.82 [8.6]	276.57 [7.9]	-126.42 [8.2]	23.75 [16.0]
C21	296.91 [15.7]	176.10 [8.5]	70.35 [14.4]	83.18 [7.5]	189.92 [16.5]	277.60 [9.8]	-127.70 [8.1]	29.91 [16.6]
C22	293.59 [22.8]	171.46 [33.0]	75.90 [30.1]	116.38 [30.3]	0.00 [0.0]	0.00 [0.0]	-127.74 [12.6]	100.08 [31.34]

Table S16: Average hydrogen bonding geometry and occupancy (considering C – O distance ≤ 3.4 Å and C-H...O angle > 120°) of possible C-H...O mediated hydrogen bond between sugar moieties of the antiparallel strands along the narrow grooves of 5'E_{GCC} and 5'E_{CGG} i-motif DNA.

C-H...O mediated hydrogen bond between sugar moiety	5'E_{GCC}			5'E_{CGG}		
	Distance between C and O (Å)	C-H...O angle (°)	Occupancy (%)	Distance between C and O (Å)	C-H...O angle (°)	Occupancy (%)
(C1) C1'-H...O4' (G22/C22)	3.30	134.89	42.86	3.28	133.52	49.45
(G22/C22) C1'-H...O4' (C1)	3.31	134.94	7.84	3.28	132.90	26.22
(C2) C1'-H...O4' (C21)	3.27	135.21	69.27	3.26	131.88	70.43
(C21) C1'-H...O4' (C2)	3.28	132.49	61.74	3.26	131.41	71.02
(C3) C1'-H...O4' (C20)	3.34	132.96	38.49	3.29	129.49	53.03
(C20) C1'-H...O4' (C3)	3.28	134.18	69.72	3.24	130.10	66.84
(C^+8) C1'-H...O4' (C^+15)	3.31	133.96	47.55	3.27	133.85	59.24
(C^+15) C1'-H...O4' (C^+8)	3.32	130.59	21.71	3.34	129.66	9.94
(C^+9) C1'-H...O4' (C^+14)	3.30	133.26	33.34	3.28	131.32	45.10
(C^+14) C1'-H...O4' (C^+9)	3.28	133.31	55.57	3.31	133.28	36.16
(G10/C10) C1'-H...O4' (C^+13)	3.39	129.73	7.21	3.34	130.08	10.10
(C^+13) C1'-H...O4' (G10/C10)	3.26	132.86	39.52	3.24	139.96	66.63

Figures:

Fig. S1: Variation of RMSD with respect to the initial energy minimized structure in case of studied i-motif systems: (a) 3'E-form structure with hemi-protonated cytosines and normal cytosines at 300K, (b) 3'E-form structure with hemi-protonated cytosines at elevated temperatures, (c) 5'E-form structure with hemi-protonated cytosines and normal cytosines at 300K, (d) 5'E-form structure with hemi-protonated cytosines at elevated temperatures, (e) 5'E_{GCC} and 5'E_{CGG}-form structure with hemi-protonated cytosines at 300K and (f) 5'E-form structure with hemi-protonated cytosines and normal cytosine at 300K with TIP3P water model.

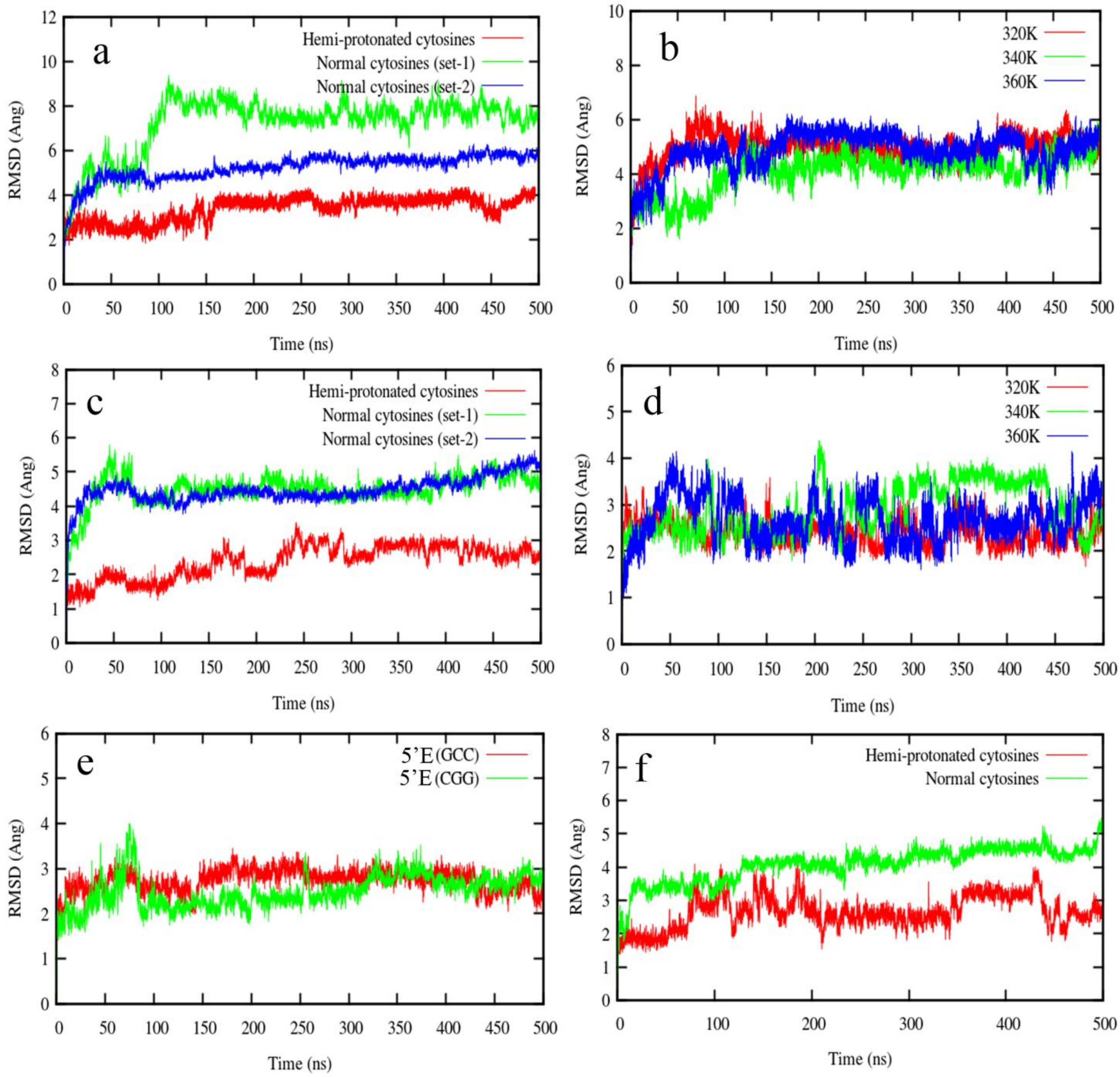

Fig. S2: Representative backbone refined conformations of model (a)-(h) $C^+C^+C^+$/CCC trinucleotide structures having different rotational orientation of intercalated base pair about its base pair helix axis and (i)-(p) tetranucleotide structures of two intercalated C^+C^+/CC dinuceotides with different helical rotations around their base pair helix axis.

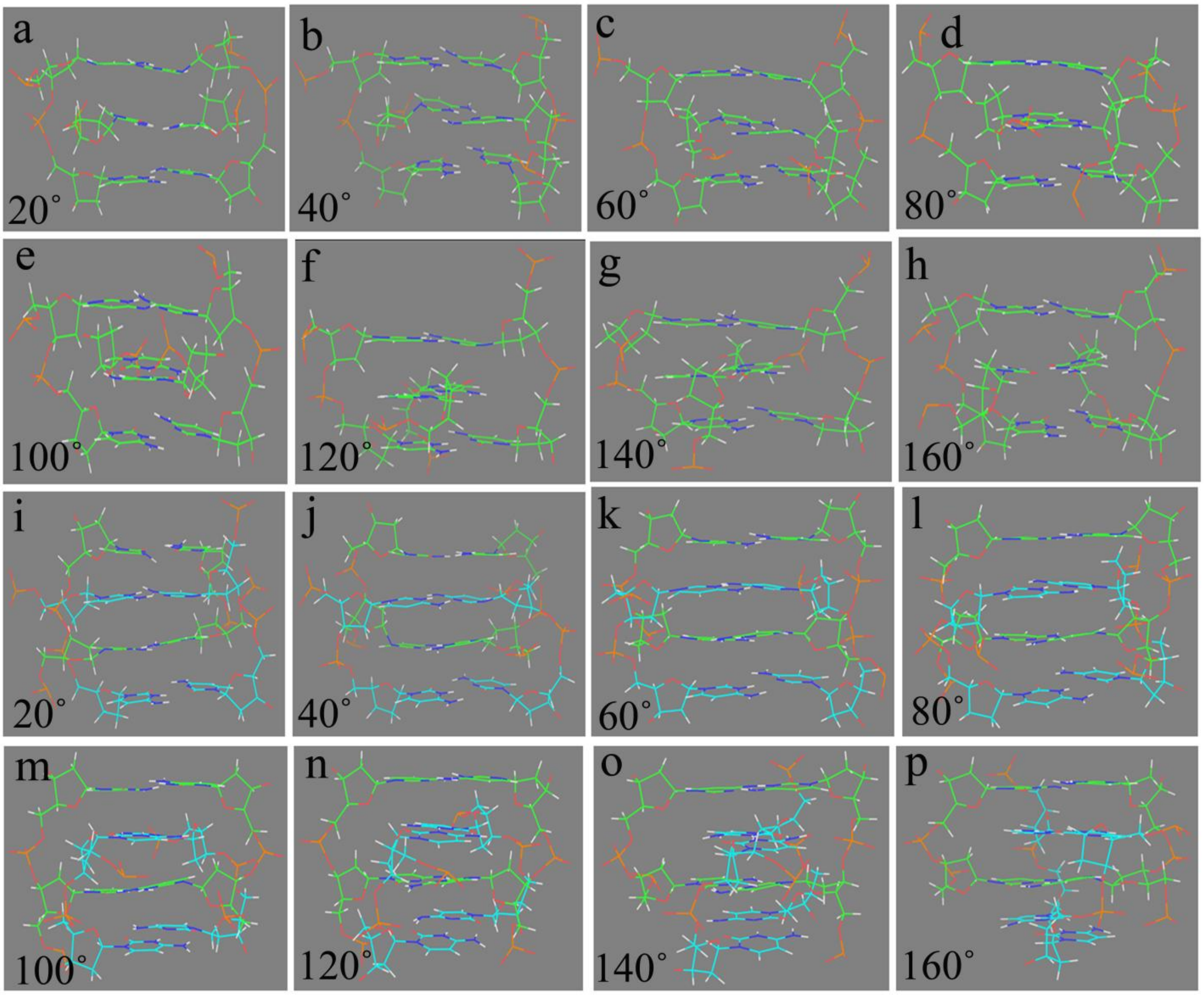

Fig. S3: Root mean square fluctuation (RMSF) of the nucleotides in (a) 3'E and (b) 5'E-form i-motif structure under acidic pH with hemi-protonated cytosines.

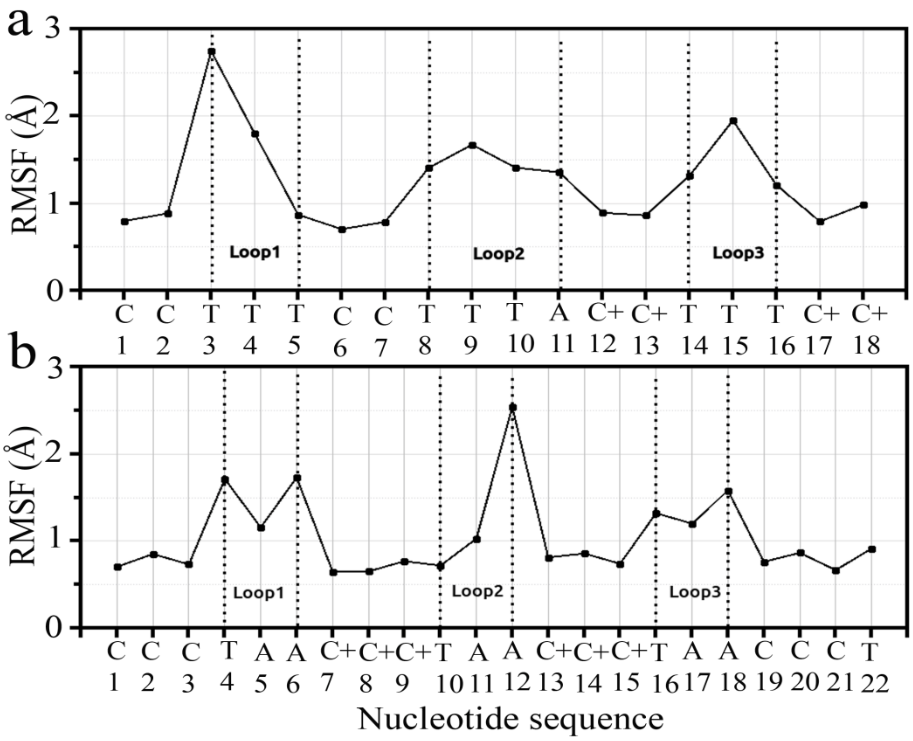

Fig. S4: Distribution of distance between the N3 atoms of paired bases in equilibrated MD trajectory of 3’E (a) and 5’E-form (b) i-motif structure with hemi-protonated cytosines, and distance matrix for the nucleobases in equilibrated conformation of 3’E (c) and 5’E-form (d) i-motif structure with hemi-protonated cytosines.

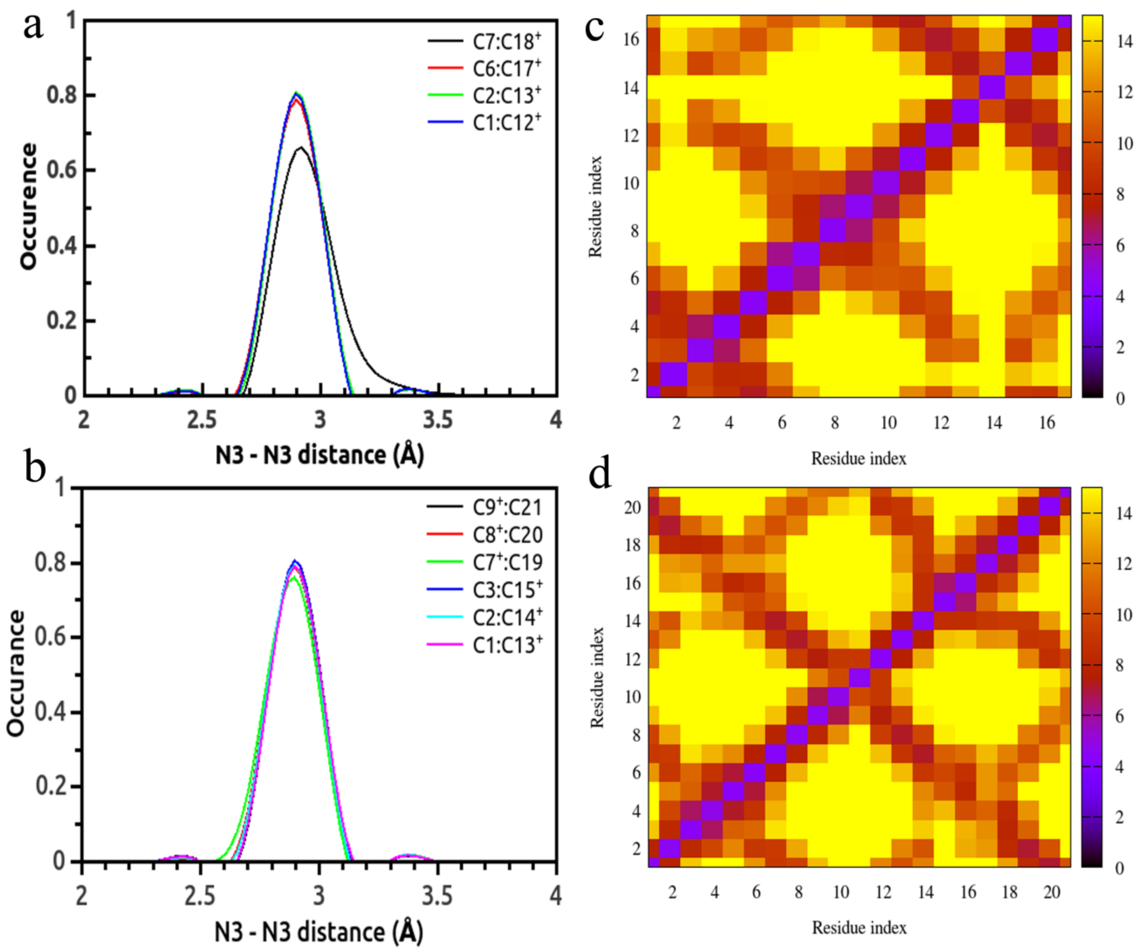

Fig. S5: Variation of distance between the N3 atoms of paired bases along the MD simulated trajectory of 3'E (a)-(b) and 5'E-form (c)-(d) structure in deprotonated state with normal cytosines.

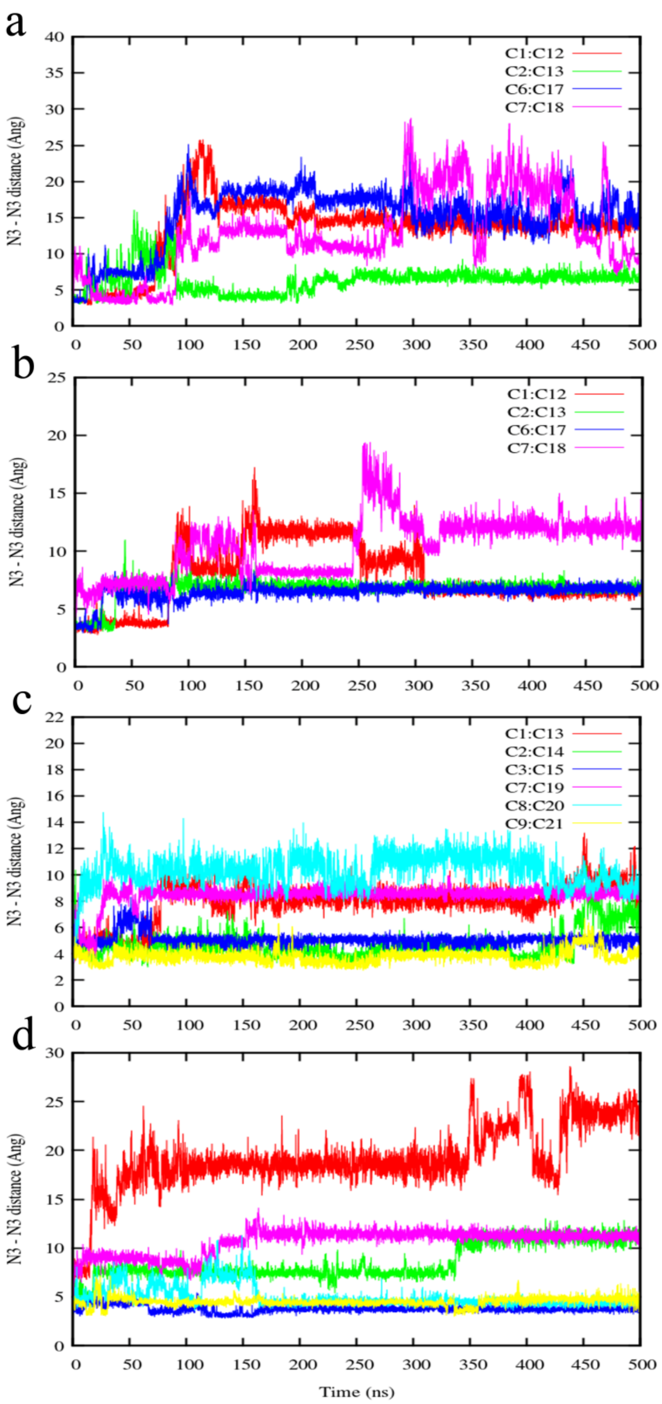

Fig. S6: Average conformation of (a) 3'E and (b) 5'E-form structure, and distance matrix for the nucleobases in equilibrated conformation of (c) 3'E and (d) 5'E-form structure under neutral pH with deprotonated cytosines.

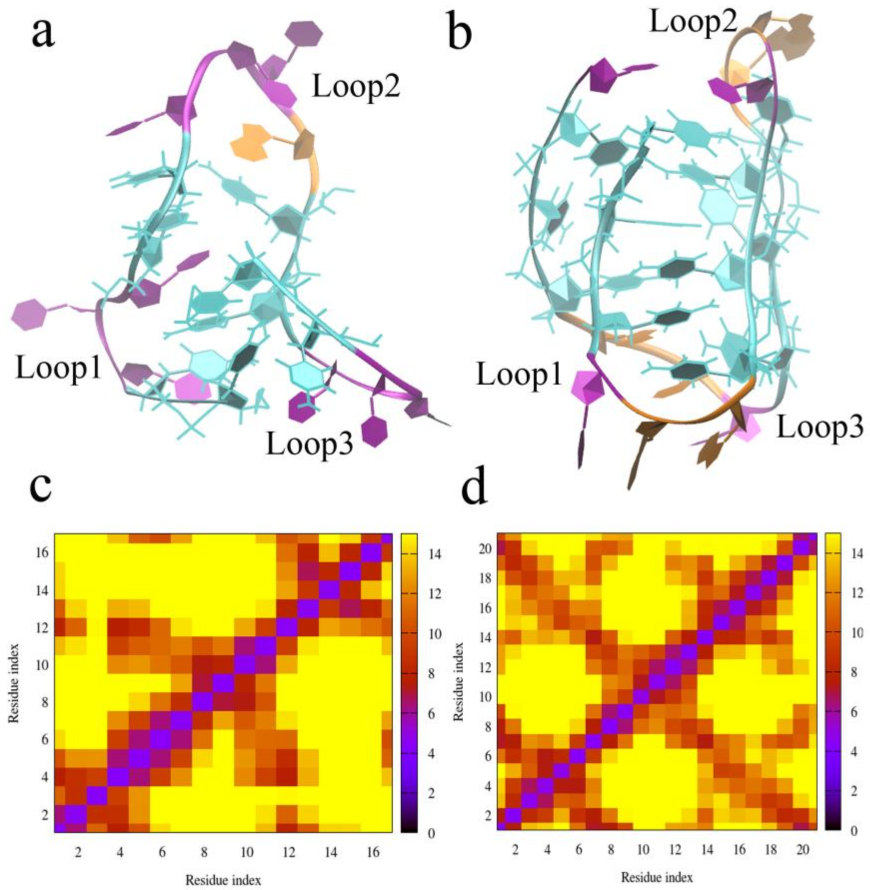

Fig. S7: Variation of distance between the N3 atoms of paired bases along the MD simulated trajectory of 3’E (a) and 5’E-form (b) structure in deprotonated state with normal cytosine considering larger simulation box, and considering TIP3P water model in case of 5’E-form structure (c).

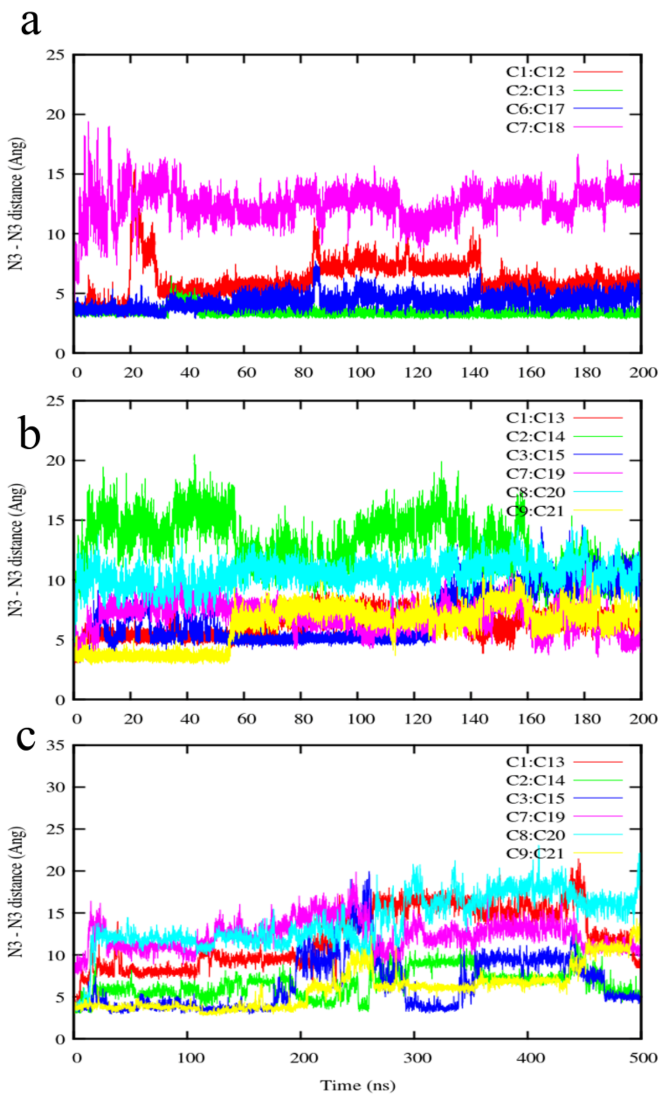

Fig. S8: 1st and 2nd normal mode of motions in the equilibrated MD trajectory of (a)-(b) 3'E and (c)-(d) 5'E-form structure under neutral pH with deprotonated cytosines.

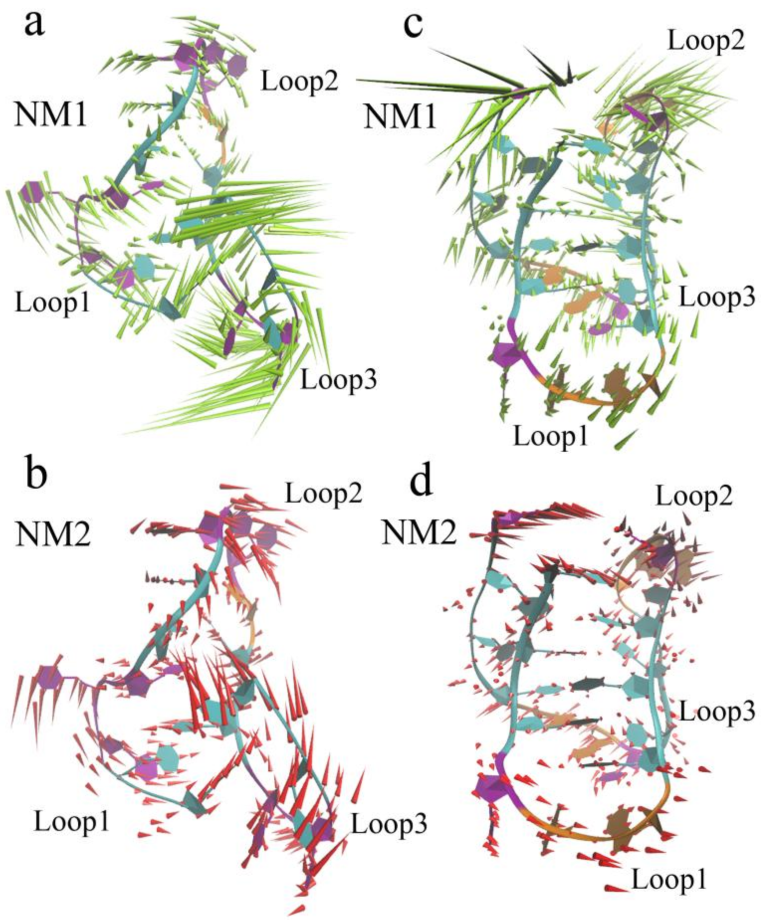

Fig. S9: Average structure of i-motif core in the equilibrated MD trajectory of (a) 3'E and (b) 5'E-form topology under acidic pH with hemi-protonted cytosines.

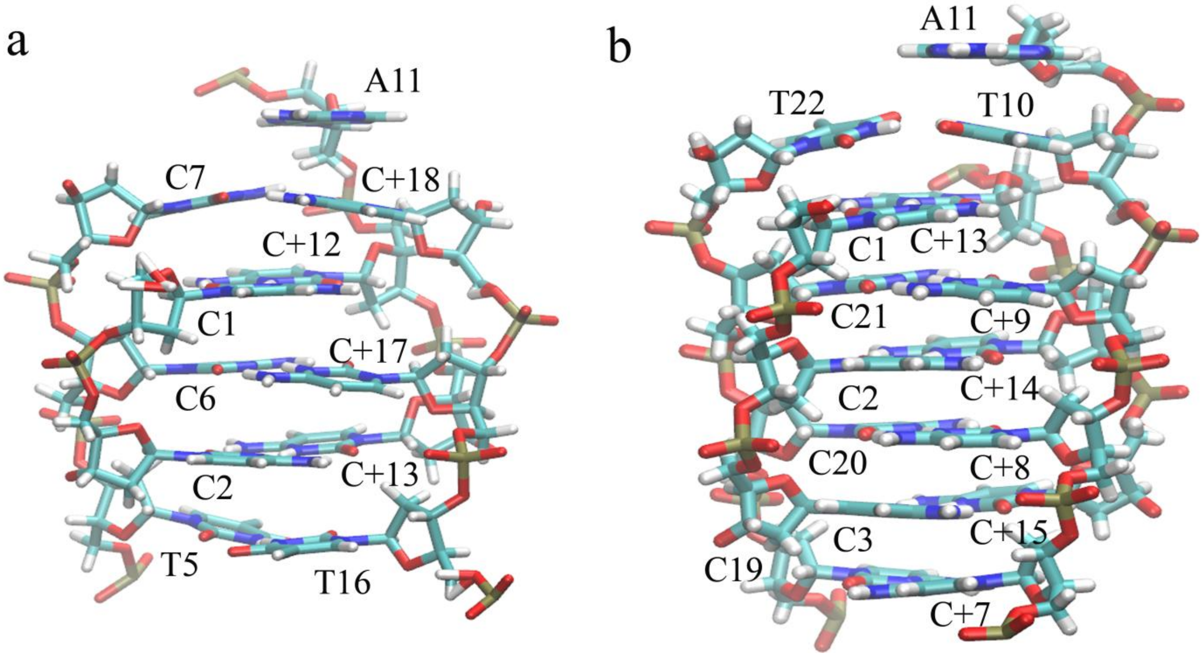

Fig. S10: Average values along with standard deviations of narrow grooves and wide grooves backbone phosphate-phosphate distances in (a)-(b) 3’E and (c)-(d) 5’E-form i-motif structure under acidic pH with hemi-protonted cytosines.

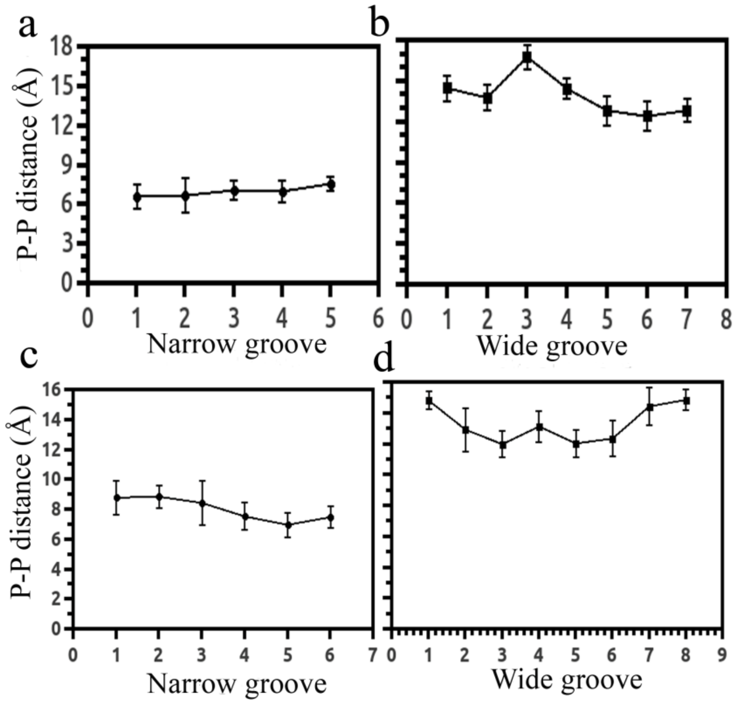

Fig. S11: Variation of energy of the sugar-phosphate backbone refined conformation of model (a) $C^{+}C^{+}C^{+}$/CCC trinucleotide structure with helical rotations (θ) of the intercalated base pair around their base pair helix axis, and (b) tetranucleotide conformations of two intercalated $C^{+}C^{+}$/CC dinuceotides with helical rotations (θ) around their base pair helix axis.

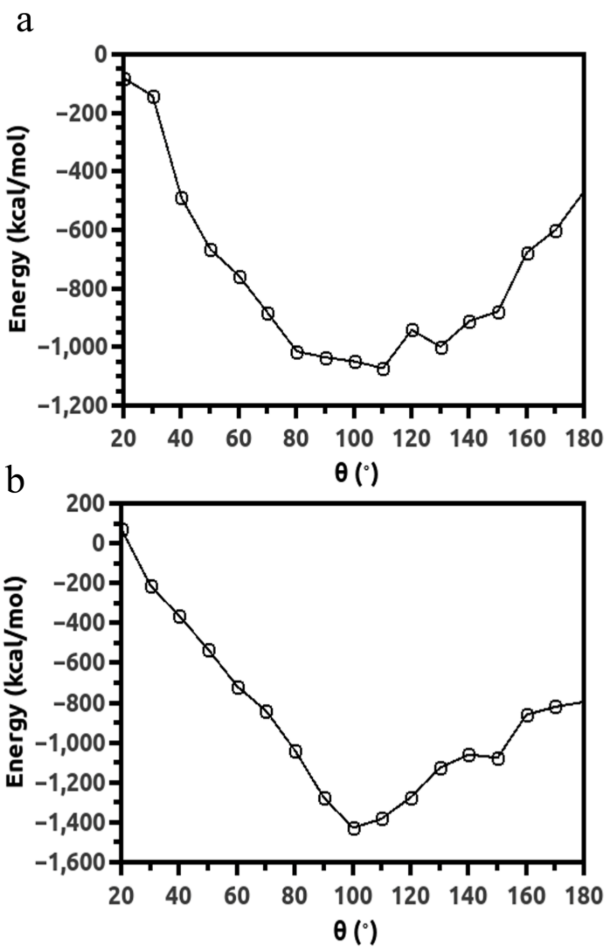

Fig. S12: Radial distributions of the oxygen (O) atom of solvent water molecule around backbone phosphate group of bases ($g(r_{P-O})$) within i-motif core with hemi-protonated cytosines under acidic pH for (a) 3'E and (b) 5'E-form structure, and in deprotonated state of cytosines under neutral pH for (c) 3'E and (d) 5'E-form structure.

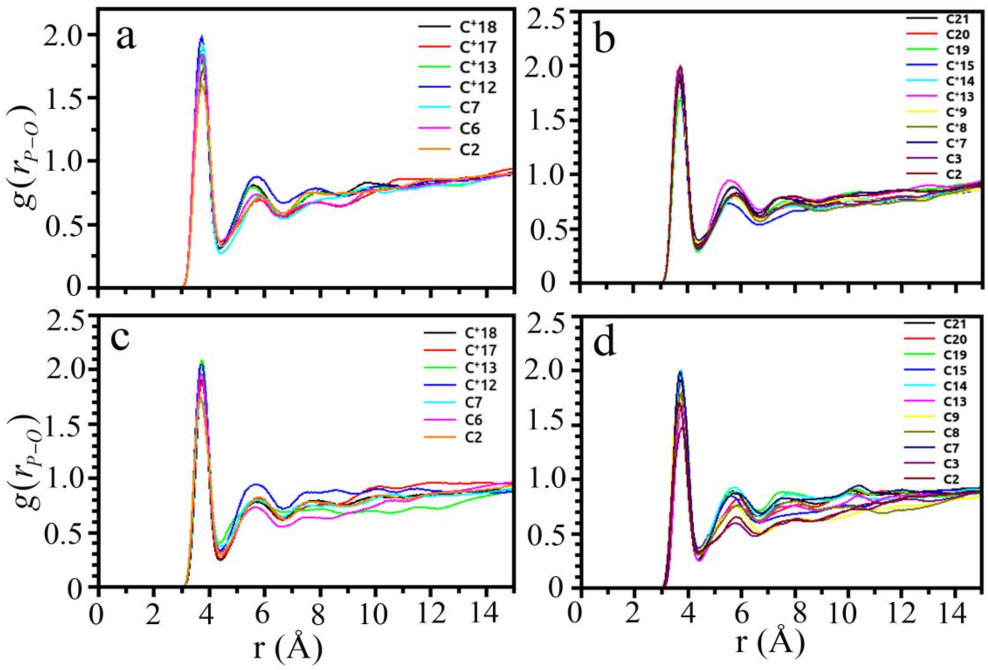

Fig. S13: Radial distributions of the oxygen (O) atoms of solvent water molecule around N4 atom of cytosines ($g(r)$) within i-motif core in hemi-protonated and deprotonated state of cytosines for (a) 3'E and (b) 5'E-form structure considering SPC/E water model, and (c) 5'E-form structure considering TIP3P water model.

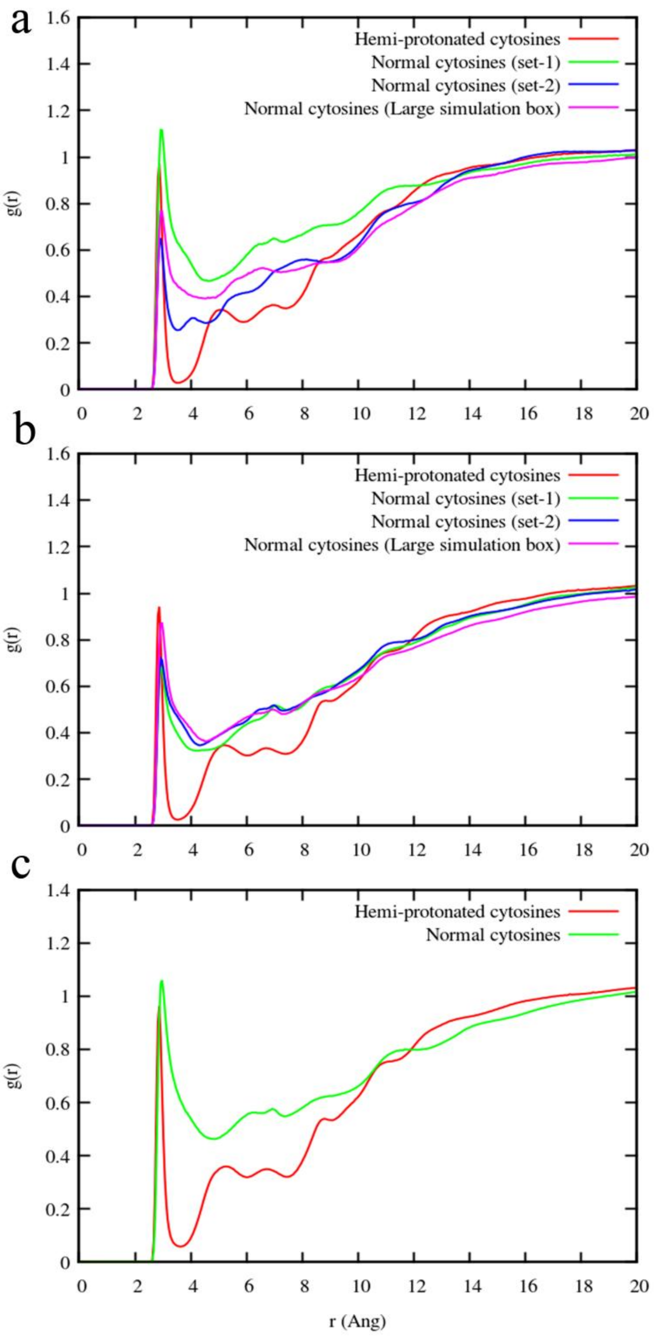

Fig. S14: Radial distributions of the oxygen (O) atoms of solvent water molecule around N4 atom of cytosines ($g(r_{N4-O})$) within i-motif core at elevated temperatures with hemi-protonated cytosines under acidic pH for (a) 3'E and (b) 5'E-form i-motif structure.

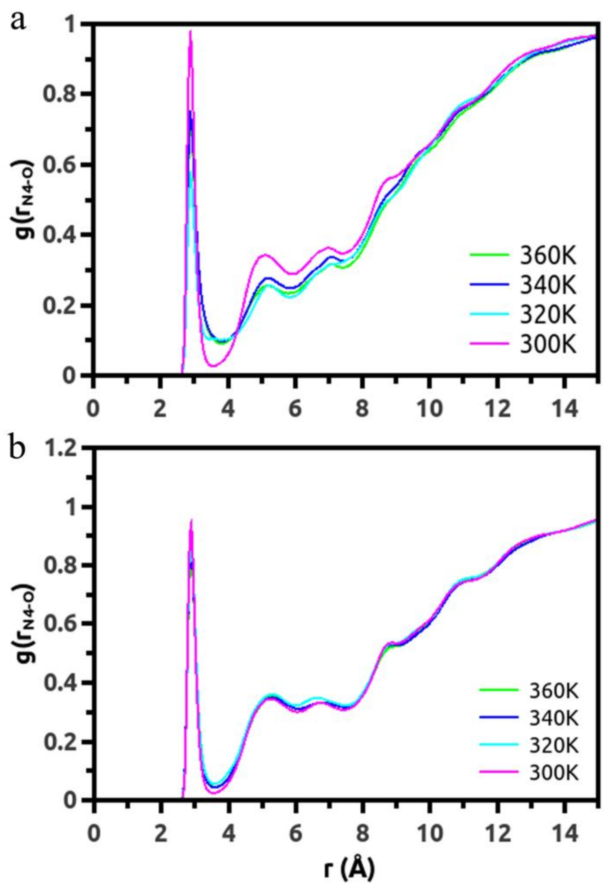

Fig. S15: (a) DFT optimized geometry of six water molecules in wider grooves first solvation cell considering MD average model conformation of $C^{+}C^{+}C^{+}$/CCC trinucleotide within the i-motif core and fixing all the non-hydrogen atoms of the bases. (b) DFT optimized structure of a water molecule along with cytosine base.

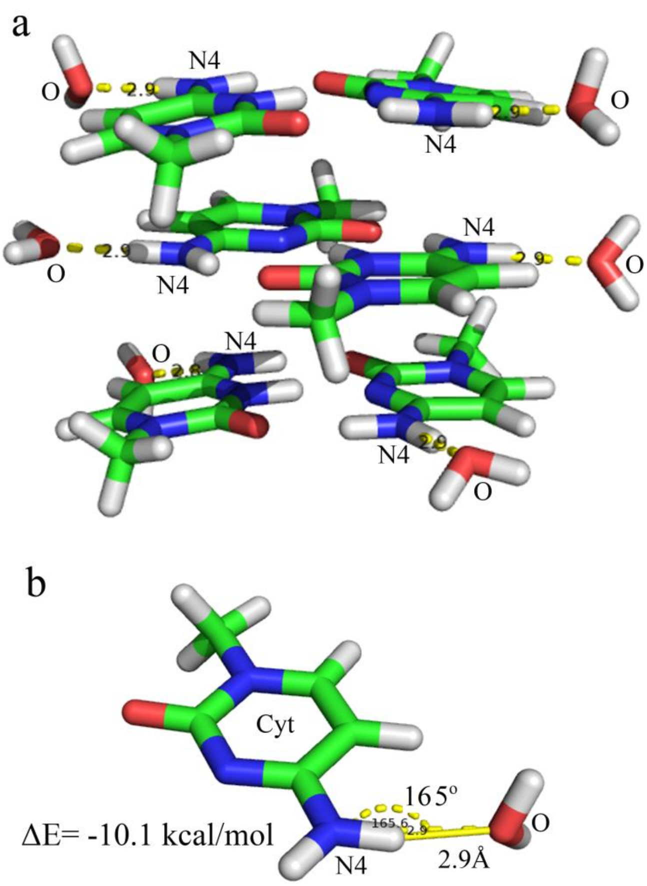

Fig. S16: First normal mode of motions at different temperature in the equilibrated MD trajectory of (a)-(c) 3'E and (d)-(f) 5'E-form i-motif structure under acidic pH with hemi-protonated cytosines.

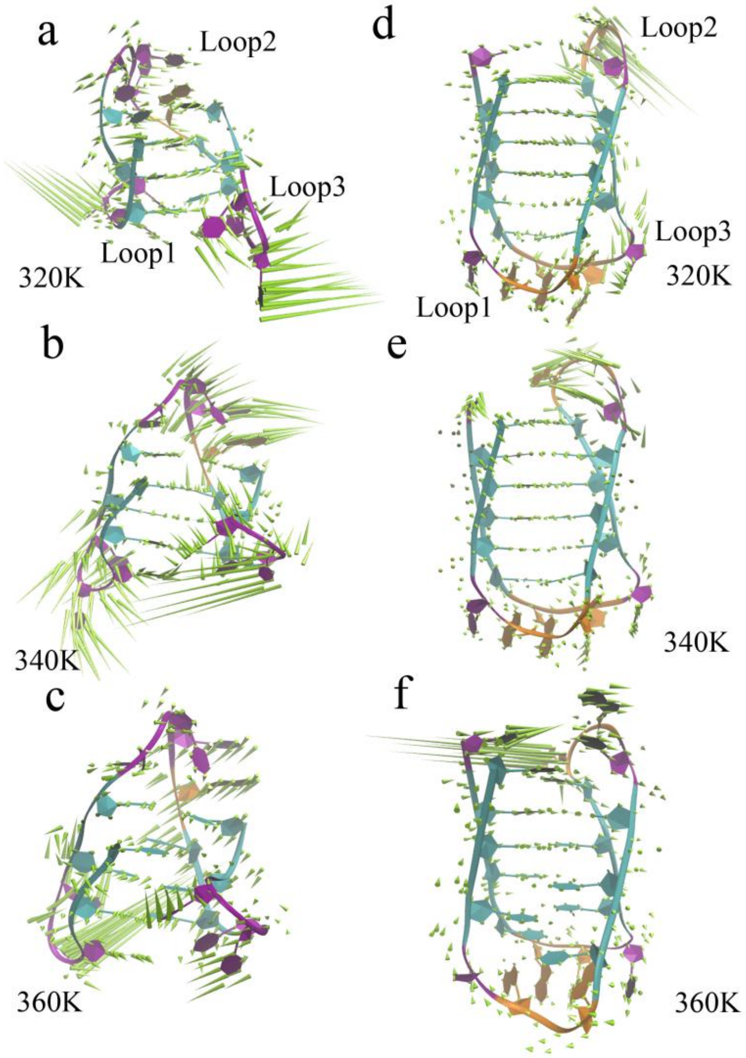

Fig. S17: Root mean square fluctuation (RMSF) of the nucleotides at different temperature in (a) 3'E and (b) 5'E-form i-motif structure with hemi-protonated cytosines under acidic pH.

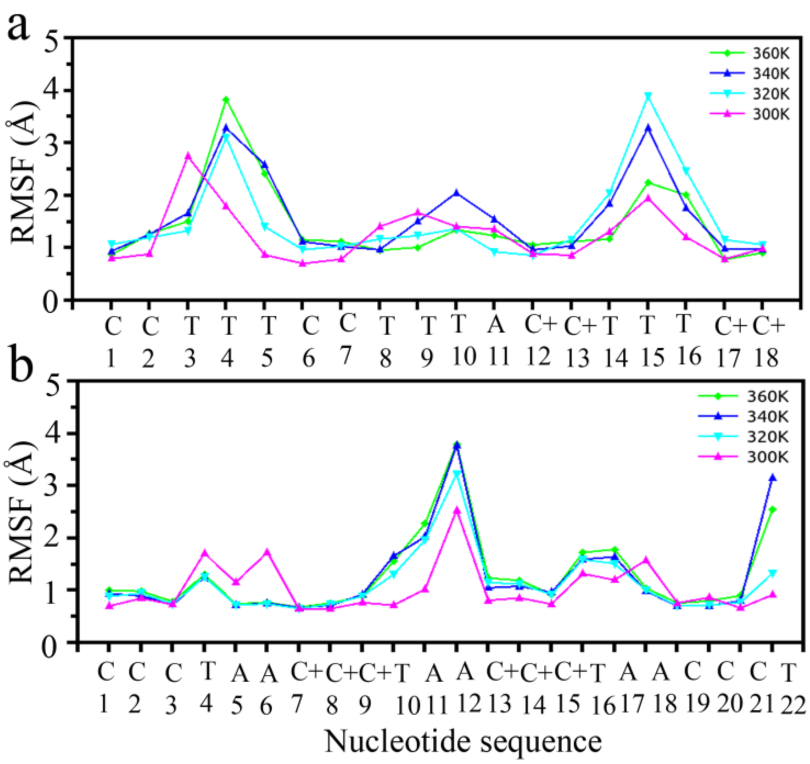

Fig. S18: At different temperature distribution of wide grooves width in (a) 3’E and (b) 5’E-form structure, narrow grooves width in (c) 3’E and (d) 5’E-form structure, and hydrogen bonding distance and angle between sugar oxygen O4' of one strand and C1' on the anti-parallel strand across the narrow grooves in (e) 3’E and (f) 5’E-form structure, as derived from the equilibrated MD trajectory of i-motif DNA under acidic pH with hemi-protonated cytosines.

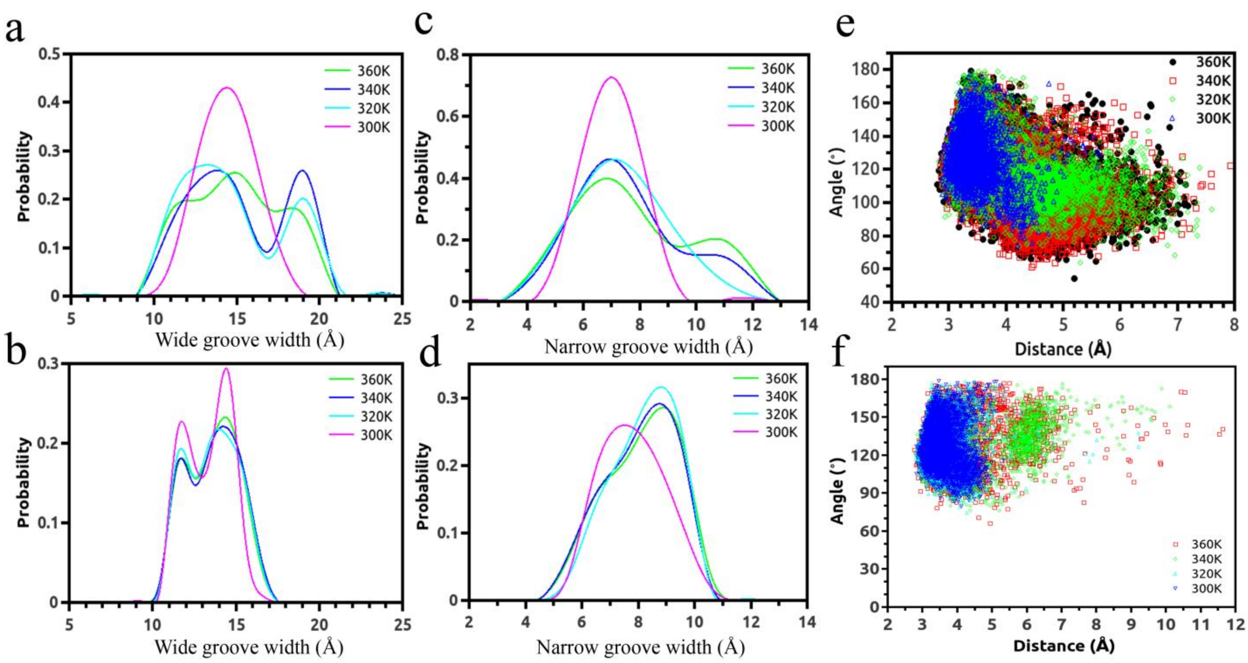

Fig. S19: Temperature dependent grid water density distribution (ρ_{wat}) around the i-motif core in (a)-(c) 3'E and (d)-(f) 5'E-form structure under acidic pH having probability of water molecules stay in that grid points greater than 0.5. Grid points are represented with a sphere of color tints wheat.

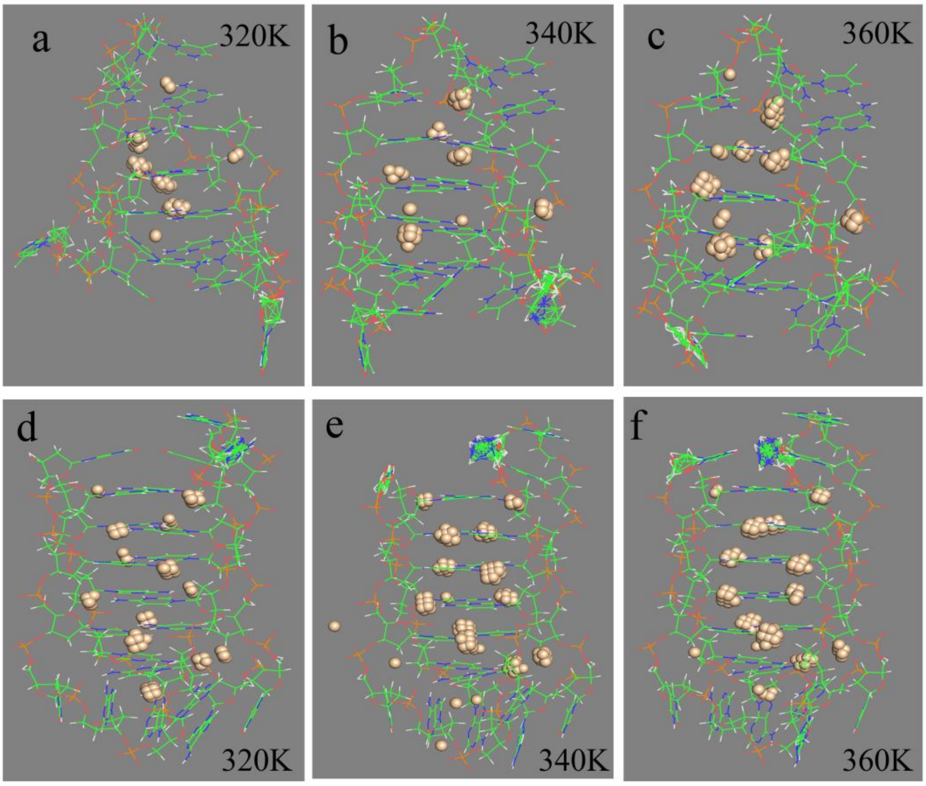

Fig. S20: (a) At different temperature distribution of number of water molecules forming hydrogen bonds with the N4 atom of cytosines in the wide grooves of 5'E-form i-motif DNA in equilibrated trajectory under acidic pH. (b) Distribution of hydrogen bonded life time at different temperature for the hydrogen bonded water molecules in the wide grooves of 5'E-form structure with hemi-protonated cytosines.

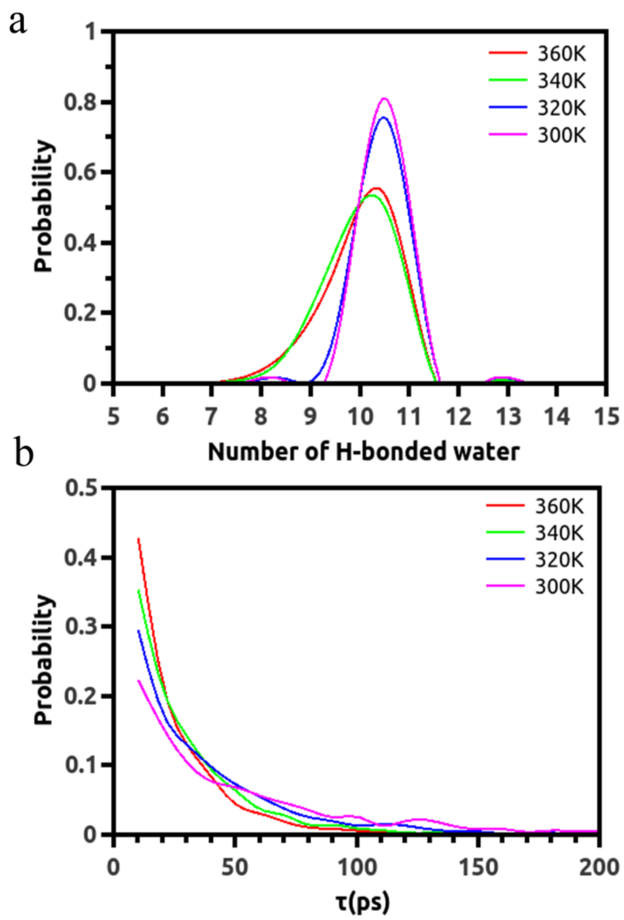

Fig. S21: In case of 5'E_{CGG} (a)-(b) and 5'E_{GCC} (c)-(d) form structure first two normal modes of motions in the equilibrated trajectory. Distribution of (e) narrow grooves width and (f) hydrogen bonding distance and angle between sugar oxygen O4' of one strand and C1' on the anti-parallel strand across the narrow minor grooves in 5'E (TAA), 5'E_{CGG} (CGG) and 5'E_{GCC} (GCC) form structure, as derived from the equilibrated MD trajectory of i-motif DNA under acidic pH with hemi-protonted cytosines.